

A STUDY OF HIGH POWER ARGON LASER OPTICS

FINAL REPORT

Contract NAS 12-548

GPO PRICE \$ _____

by

CFSTI PRICE(S) \$ _____

George de Mars

Michael Seiden

and

Frank Horrigan

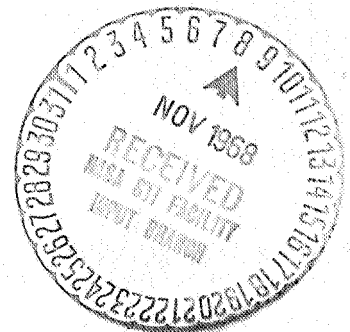
Hard copy (HC) _____

Microfiche (MF) _____

ff 653 July 65

RAYTHEON COMPANY
Research Division
Waltham, Massachusetts

AUGUST 1968



Prepared for
Electronics Research Center
NATIONAL AERONAUTICS AND SPACE ADMINISTRATION

N 68-37855

(ACCESSION NUMBER)

(THRU)

58
(PAGES)

(CODE)

CR-86111
(NASA CR OR TMX OR AD NUMBER)

(CATEGORY)

FACILITY FORM 602

Mr. Harry Ceccon
Technical Monitor
NAS 12-548
Electronics Research Center
575 Technology Square
Cambridge, Massachusetts 02139

Requests for copies of this report should be
referred to:

NASA Scientific and Technical Information Facility
P. O. Box 33
College Park, Maryland 20740

A STUDY OF HIGH POWER ARGON LASER OPTICS

By George deMars, Michael Seiden, and Frank Horrigan

Final Report

April 15, 1967 to April 14, 1968

August 1968

Prepared under Contract No. NAS 12-548 by
RAYTHEON COMPANY, RESEARCH DIVISION
Waltham, Massachusetts

Prepared for
Electronics Research Center
NATIONAL AERONAUTICS AND SPACE ADMINISTRATION

TABLE OF CONTENTS

	Page
SUMMARY	1
INTRODUCTION	1
APPARATUS AND MATERIALS	5
Laser Structures	5
Optical Components	7
TEST RESULTS	14
Degradation of the Windows	14
Aging of the Structure	17
Influence of the Laser Beam on the Rate of Degradation	17
Direct Detection of Optical Damage	20
Cathode vs Anode	20
Window Mounting and Cleaning Procedures	23
Discharge Structure Erosion	24
Principal Laser	24
Graphite Laser	25
Transport Studies	28
Counter Measures	33
Heating	33
Sputtering	34
Mirror Heating	38
Evaluation of Available Commercial Mirrors	38
Notes on Tests	40
DISCUSSION AND CONCLUSIONS	42
REFERENCES	51
NEW TECHNOLOGY APPENDIX	52

PRECEDING PAGE BLANK NOT FILMED.

LIST OF ILLUSTRATIONS

Number	Title	Page
1	Typical Decay of Output Power Due to Window Degradation. Discharge Current is 70 Amperes	3
2	Mode Distortion of Argon Laser (70 A Discharge)	4
3	The Principal Laser	6
4	Schematic of Argon Laser	8
5	Anode End of Principal Laser, Stopcock and Tunable Mount for Vacuum Optics	9
6	Side View of Anode End of the Principal Laser	10
7	Vacuum Window and Mirror Mounts	11
8	The Segmented Pyrolytic Graphite Bore Laser	12
9	Schematic Diagram of Pyrolytic Graphite Bore Laser	13
10	Arrangement of Apparatus for Obtaining Shearing Interferograms of Brewster Angle Window	15
11	Shearing Interferograms of Brewster Angle Window During Laser Operation	16
12	Comparison of Decay Rates of Laser Output Due to Window Degradation for Old and New Discharge Structures	18
13	Change in Output Power Decay with Use of Discharge Structure	19
14	Output Power Decay Using Windows Previously Exposed to Lasing and Nonlasing Discharge	21
15	Fog Pattern Produced on Cooled Mirror Surface after Exposure to Lasing Discharge	22
16	Location of Deposit at Cathode End of Discharge Tube	26
17	Schematic Diagram of Pyrolytic Graphite Bore Laser	27
18	Potential Gradient in Plasma Region Beyond Anode vs Discharge Current (Principal Laser)	29

LIST OF ILLUSTRATIONS (Cont'd)

Number	Title	Page
19	Potential Gradient in Plasma Region Beyond Cathodes vs Discharge Current (Principal Laser)	30
20	Particle Flow Observed with Voltage Gradient Established between End Flange and Anode	31
21	Particle Transport in the Region between the Anode and the End Bellows. Anode-Bellows Potential Difference 600V. a) No potential gradient. b) Gradient established: Particle streaming. c) Gradient removed: Particle dispersal.	32
22	Effect of Argon Sputtering of Degraded Window on Output (Pyrolytic Graphite Bore Laser, Argon Pressure 450 M Torr)	35
23	RF Discharge Used for the Restoration of Terminal Optics	36
24	Effect of RF Discharge on Output (Principal Laser)	37
25	Bulk Temperature of End Mirrors Monitored During Laser Operation	39

A STUDY OF HIGH POWER ARGON LASER OPTICS

By George deMars, Michael Seiden, and Frank Horrigan

SUMMARY

The development, over the past several years, of high power, continuous duty, argon ion lasers has encountered limitations in the form of a severe optical degradation problem. An absorbing film builds gradually on the optical components which terminate the discharge tube. This layer absorbs a small fraction of the laser power, thermally distorts the optical components, and unbalances the optical cavity. In this way the laser power that can be extracted is limited to some value far below the inherent capabilities of the active medium.

Experimental investigations of Brewster-angle window degradation were performed on a large quartz bore laser capable of cw powers in excess of 100 watts. Methods of recognizing and measuring the extent of window damage were established. Contaminants generated by the discharge erosion of the electrodes and the bore structure proved to be the source of the problem. Studies of the transport processes suggested that the motion of charged particles under the influence of the plasma fields is the dominant mechanism by which the contaminants reach the terminal optics. On the basis of the understanding achieved during this study, various techniques to modify or prevent the degradation were developed and assessed.

INTRODUCTION

With the continued advance of ion laser technology has come the recognition of certain persistent obstacles to long-life, high-power performance. Adequate structures capable of tolerating the high thermal loadings required have been developed in a wide variety of forms. Hence, outright destruction of the laser by thermal overload no longer poses a serious threat. At the present time the real limitation to the useful life of an ion laser seems to be in the optical component. All ion laser types fabricated to date - from conduction-cooled dielectric tubes of quartz or ceramic, through various metal-insulator stack assemblies, to radiation-cooled systems using graphite or metal disks or slugs - have exhibited progressive degradation of the terminal optics which eventually limit the output power to values far below those obtained from the structure when new.

These effects were first noticed in our laboratory several years ago when argon ion discharge structures, capable of continuous operation

with circulating cavity power densities in excess of 1 kW/cm^2 , were constructed. Operation of these structures revealed deficiencies in the capability of the optical components to accommodate such power levels.

The multiple-layer dielectric mirrors available at this time not only became thermally distorted during laser operation, but often suffered permanent damage in the form of film "bleaching" or actual film disruption. The mirror damage problem was particularly acute when the mirrors were placed at a terminal end of the discharge structure.

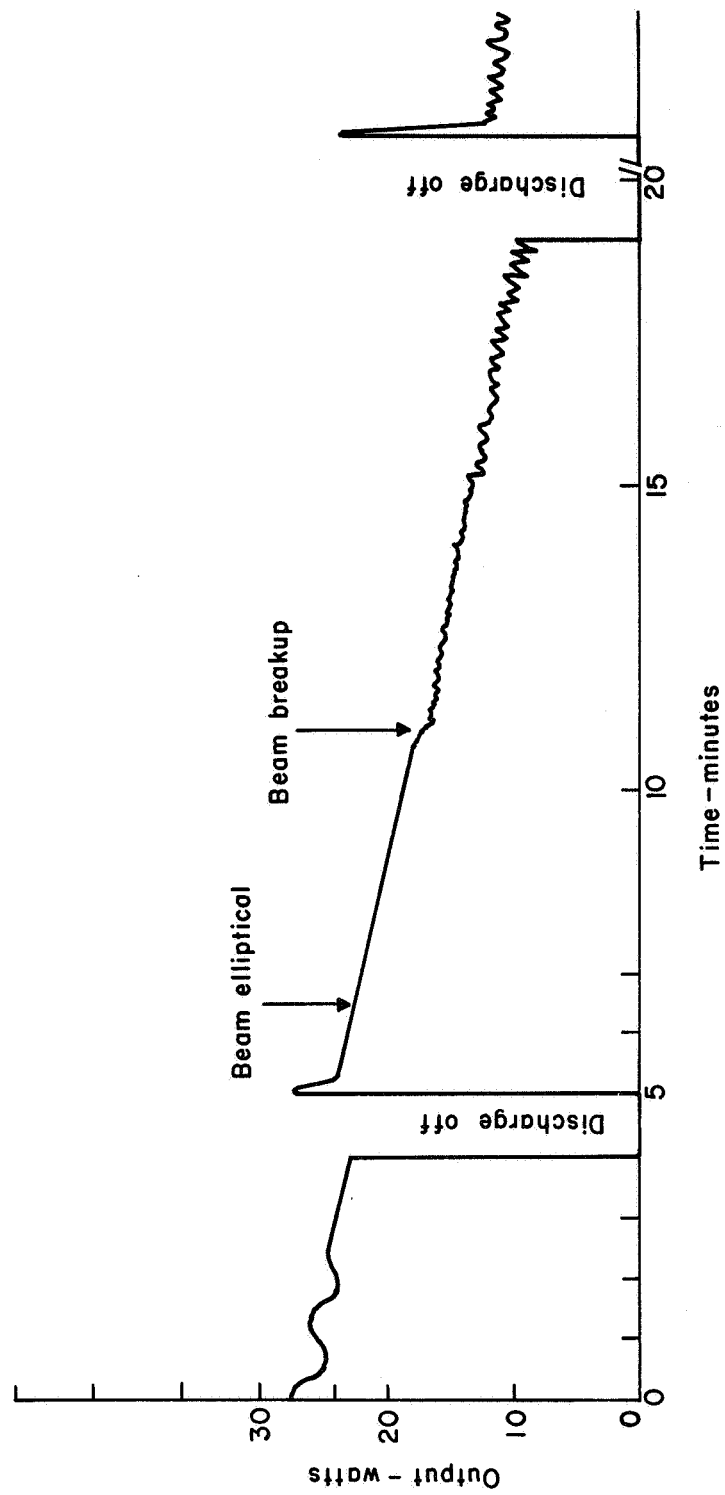
Even more troublesome were the power-limiting effects encountered when a Brewster-angle window was used at the termination. In this case, laser output was found to decay with time at a rate which varied with the level of operation: the higher the current, the faster the decay. Figure 1 illustrates the decay in output power observed when such a configuration was employed with a large bore (8mm) quartz discharge tube. A shrinking of the beam size and a change in mode configuration were observed to be coincident with this power decay. These changes occurred in a regular sequence: an initial reduction in beam diameter was followed by a shift from circular to elliptical cross section as shown in Fig. 2, photos 1 - 3. As is shown in photos 4 - 6, further beam shrinkage continued until a series of abrupt changes in mode geometry occurred; these are noted on the plot in Fig. 1 as "beam breakup." Eventually an equilibrium condition would be established in which both the output power and beam area were only a fraction of the original values. If lasing were interrupted at this point by masking one of the mirrors and later resumed, a rapid re-enactment of the above-described cycle ensued, as depicted in that portion of the plot in Fig. 1 beyond the 20-minute mark.

The power decay rate after installation of fresh mirrors and/or windows varied widely among various discharge structures. However, for a given structure the power decay rate was severely dependent on discharge current and optical power density.

Such were the observed limitations of high power, ionized argon laser operations at the initiation of this contract. It was recognized then that most of the output power degradation resulted from thermal distortion of the optical components in the cavity due to increased absorption of the lasing radiation. However, the site of this absorption and the mechanism by which it was induced were not understood.

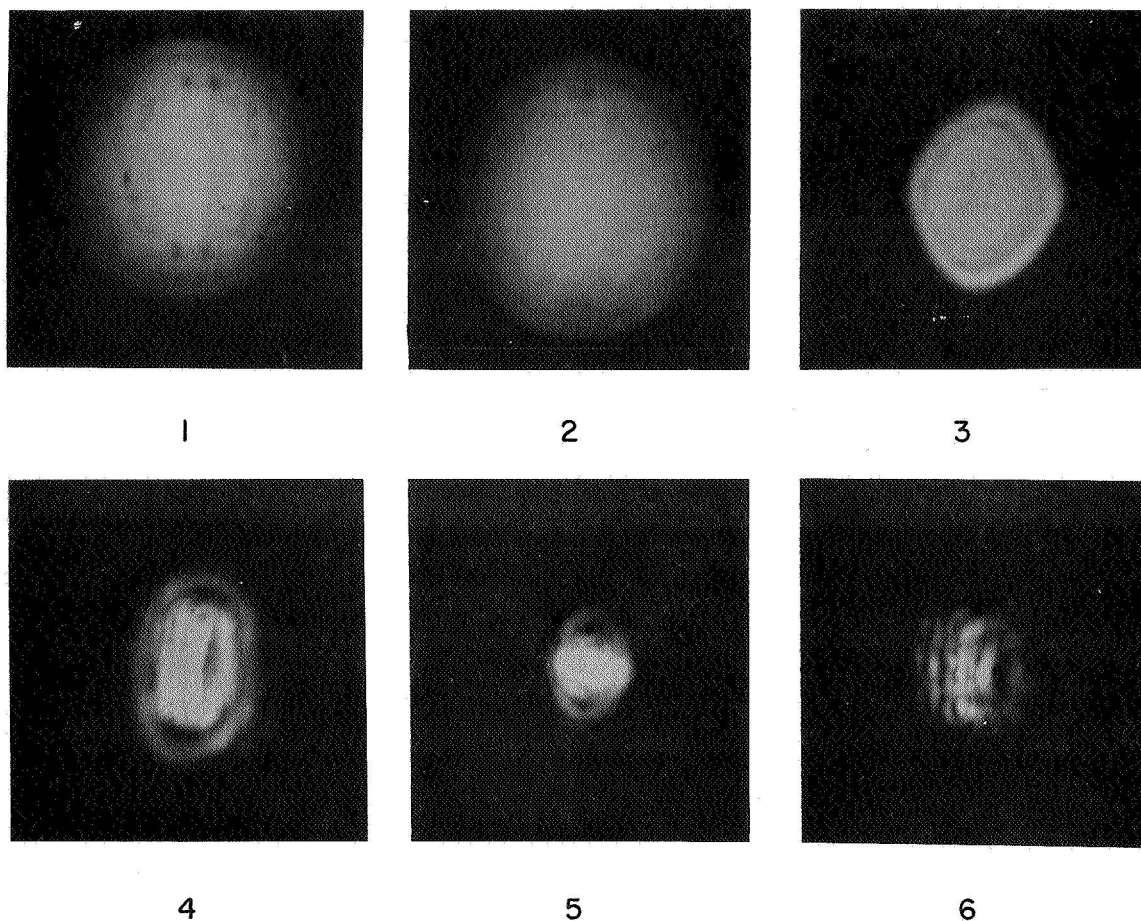
A number of agents which might be capable of modifying the optical characteristics of the components were considered:

1. Nonlinear effects produced by the continuous high optical power density.
2. Color centers formed by the vacuum UV produced in the ionized discharge.



TYPICAL DECAY OF OUTPUT POWER DUE TO WINDOW DEGRADATION. DISCHARGE CURRENT IS 70 AMPERES.

FIGURE 1



MODE DISTORTION OF ARGON LASER
(70 A Discharge)

- 1 Laser turned on 15 W output
- 2 After 1 minute 10 W output
- 3 After 5 minutes 9.3 W output
- 4 After 10 minutes 7.5 W output
- 5 After 20 minutes 6.5 W output
- 6 After 35 minutes 5 W output

FIGURE 2

3. An optically absorbing surface layer produced by either a) an alteration of the surface structure itself, or b) a deposit of material released within the discharge structure.

In order to exploit the advances in high density ionized argon discharge tube construction, this investigation was undertaken to determine the nature and cause of optical component failure under conditions of high power. In addition, remedial methods were assessed experimentally with a view toward eventual attainment of argon laser, single transverse mode output power levels in excess of 30 W.

Optical component tests in this study were made utilizing a large ionized argon discharge structure which, when operated as a laser, has an output power capability approaching 100 W. With this structure, component behavior was observed at high power levels under practical laser operating conditions.

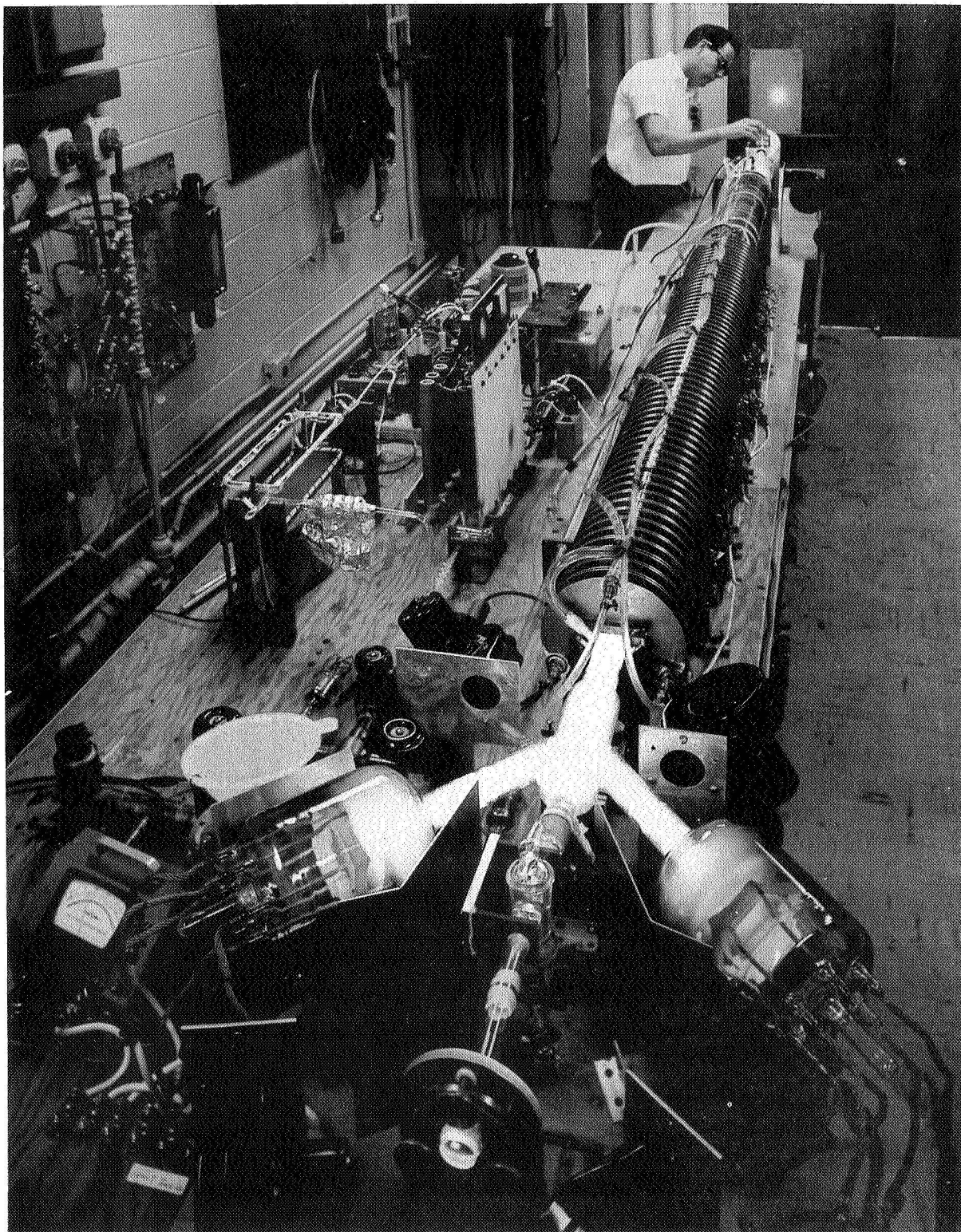
Initial experiments were directed primarily toward understanding the nature of optical window degradation. Methods of identifying and measuring the extent of window degradation were developed. The extent and rate of degradation were determined for various cavity configurations and discharge operating levels. Various techniques to modify or prevent the degradation were developed.

In addition to the investigation of the progressive degradation phenomenon, an evaluation of state-of-the-art dielectric-coated mirrors for use in high output power operation was made. Seven vendors of such mirrors were contacted and their best-effort results were tested under actual high power operation and compared with each other.

APPARATUS AND MATERIALS

Laser Structures

The discharge structure used for most of the work performed in this investigation is shown in Fig. 3. The ionized argon discharge is produced in a water-cooled quartz tube about 270 cm long and 8 mm in diameter. An external by-pass is employed. The multiple, oxide-coated, nickel mesh cathodes have a total rated capacity of 200 A. A remote power supply rated at 200 A and 750 V provides high current operation of the tube. Axial magnetic fields up to 1 kOe are provided by solenoids encompassing the length of the tube. Large bore, in-line stopcocks are used in conjunction with a large capacity pumping system to provide isolation of the terminal optics,



THE PRINCIPAL LASER
FIGURE 3

which permits rapid, easy interchange of the optics without disturbing the electrodes. A typical optical cavity configuration is shown schematically in Fig. 4. The optics are mounted, using O-ring seals, on a positioning structure connected by metal bellows to the discharge tube. Detailed views of the valving and tuning arrangement at the anode end of the discharge structure are shown in Figs. 5 and 6. Some details of the Brewster-angle window and internal mirror mounts are indicated schematically in Fig. 7 at parts A and C.

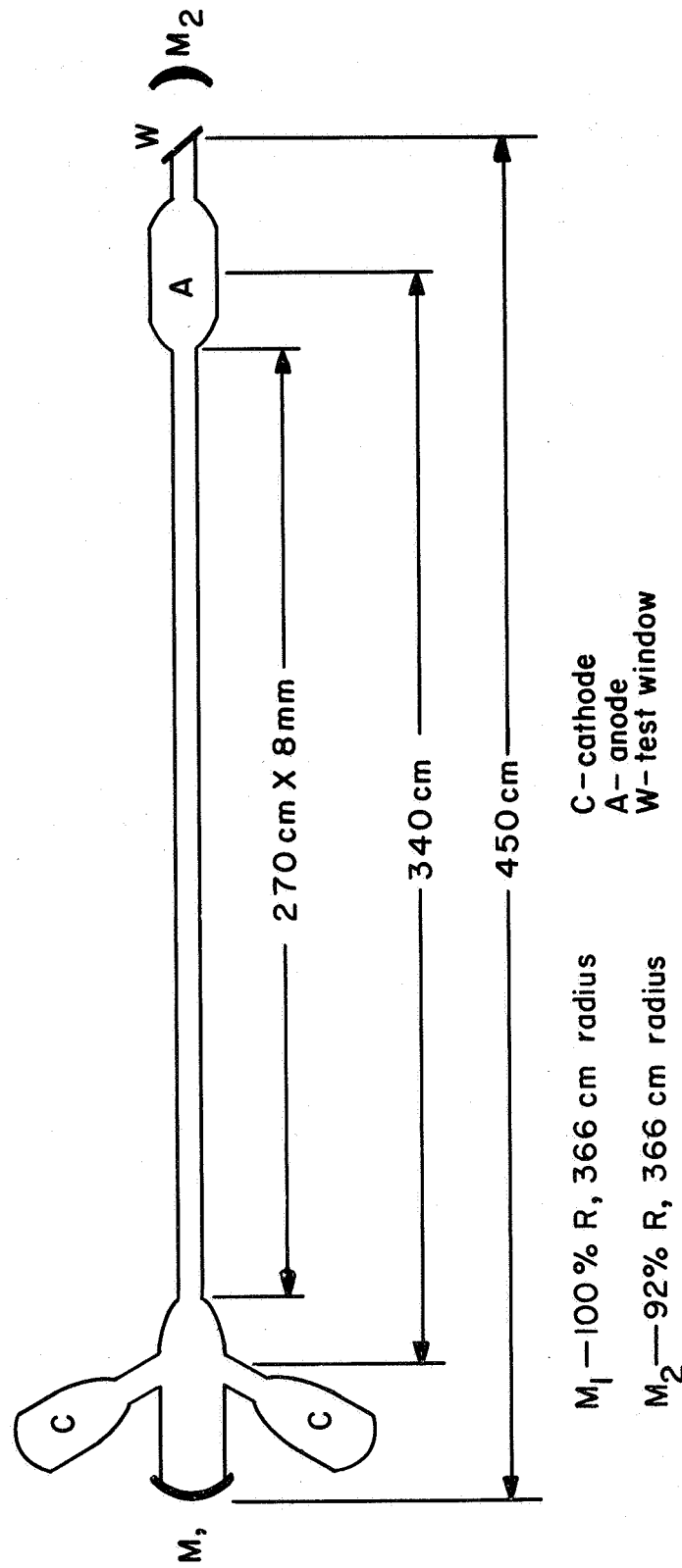
A pyrolytic graphite bore structure, shown in Fig. 8, also was used in the course of this investigation. Figure 9 is a schematic diagram of this device. The segmented bore formed by the graphite elements is 3 mm in diameter and 23 cm long. The radiation-cooled slugs, separated and aligned by pyrolytic boron nitride pins, are 2.5 cm thick and have an outer diameter of 4 cm. A water jacket (not shown) which provides a heat sink encompasses the quartz envelope. A solenoid (not shown) is used to provide axial magnetic fields up to 800 Oe. The cathodes have a total rated capacity of 100 A. The dc discharge is powered by a 1500 V, 80 A supply. An output power of 4.5 W has been achieved with a 60 A discharge. In-line gate valves are provided to facilitate the interchange of the terminal optics.

Each of these argon structures is provided with interconnected pumping and gas handling systems. A liquid nitrogen cold trap is located at the junction of the systems. Fill pressures were monitored with appropriate pressure gauges. Laser output power was monitored using a calorimeter (calibrated with a commercial power meter) and chart recorder.

Optical Components

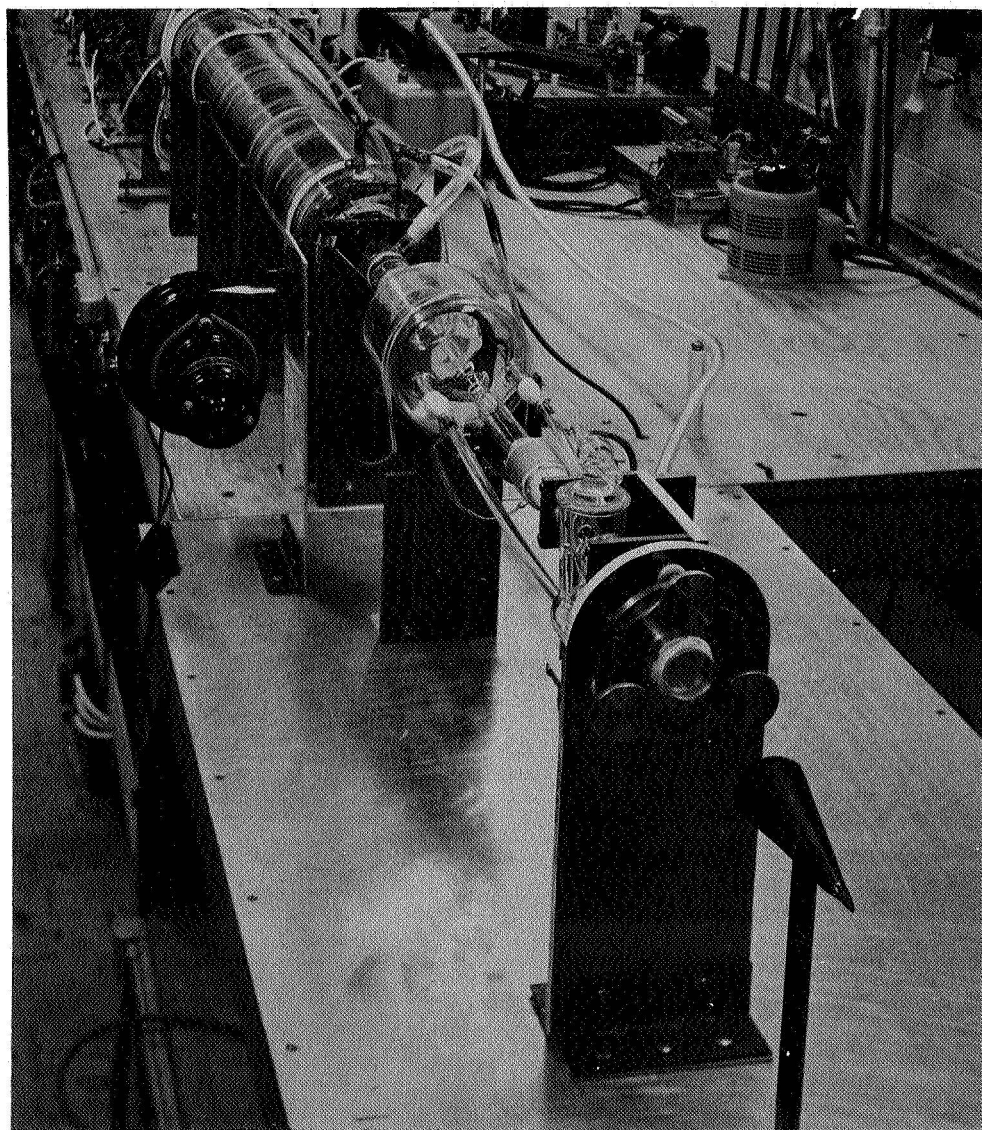
The initial supply of optical flats used for Brewster-angle windows was obtained from a number of vendors. These flats were fabricated from highest grade, fused synthetic quartz (e.g., Suprasil grade from Amersil, Inc.) and were specified to be flat to better than $1/10$ wave with a minimum light scatter finish. Acceptance tests were performed and subsequent acquisitions of flats were made from those vendors who had provided a finish with the least amount of light scatter.

All mirrors used to date were made of multilayer, dielectric coatings on fused quartz substrates. Three different radii of curvature of 3.7, 6.6, and 10 m, all finished to at least $1/10$ wave, were employed in pairs of similar geometry. Most of the mirror testing, however, was done with 3.7 m radius mirrors. In this effort we have received excellent cooperation from seven leading vendors, five of whom are located in the Northeast and two on the West Coast. In most cases best-effort coating procedures were employed, at no charge, on the identical substrates provided.



SCHEMATIC OF ARGON LASER

FIGURE 4



ANODE END OF PRINCIPAL LASER, STOPCOCK
AND TUNABLE MOUNT FOR VACUUM OPTICS

FIGURE 5

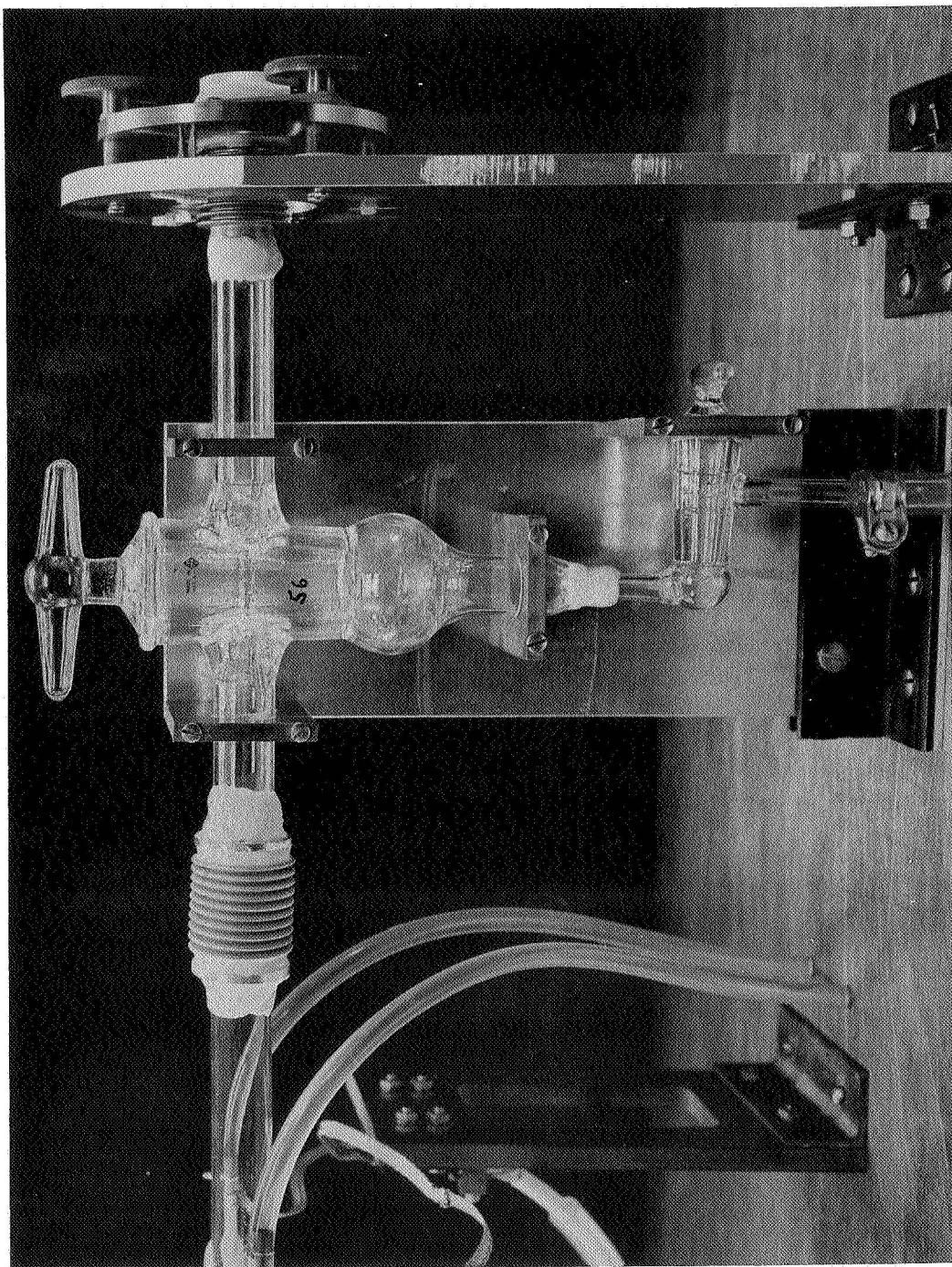
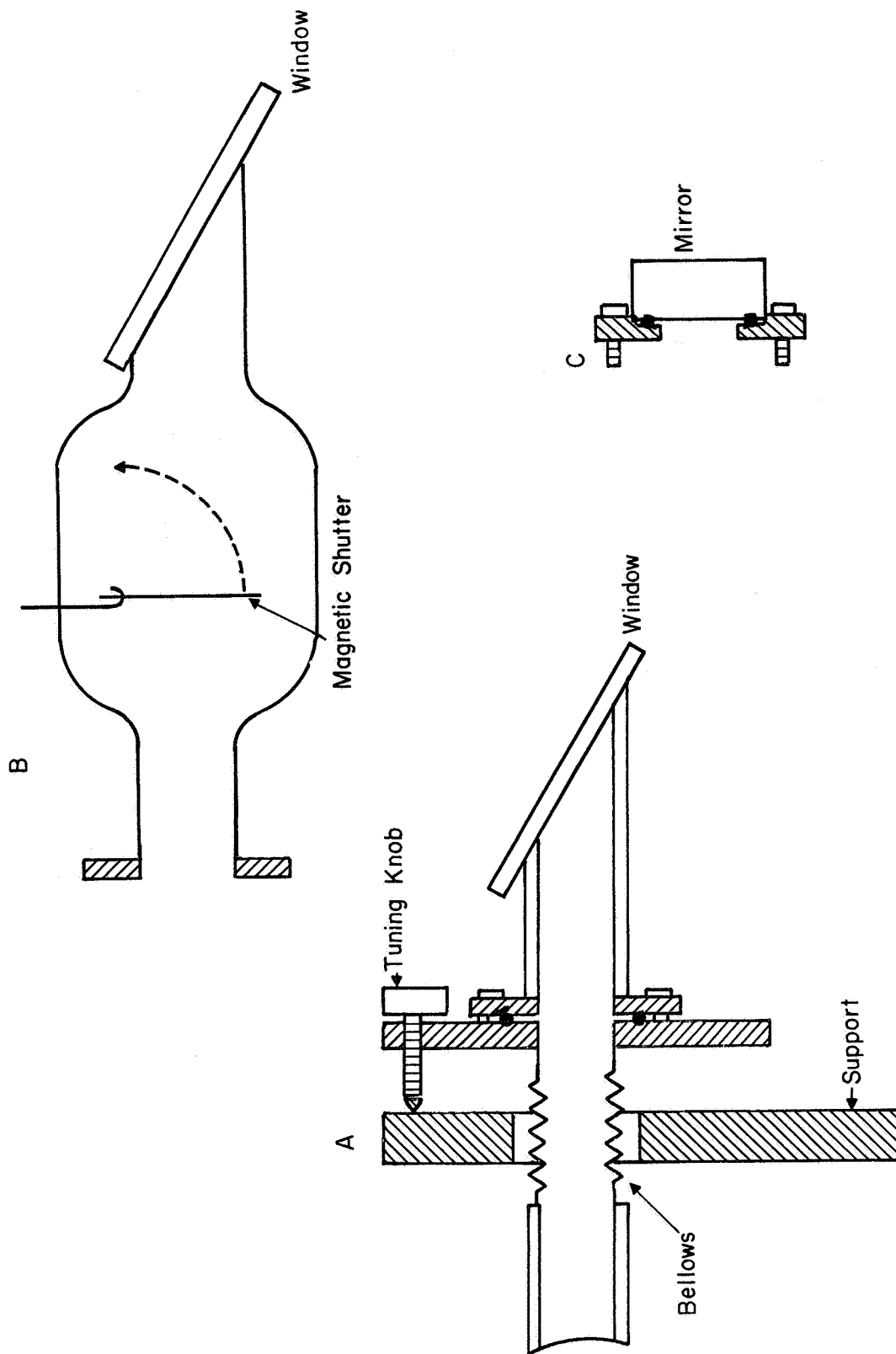


Fig. 6 Side View of Anode End of the Principal Laser



VACUUM WINDOW AND MIRROR MOUNTS

FIGURE 7

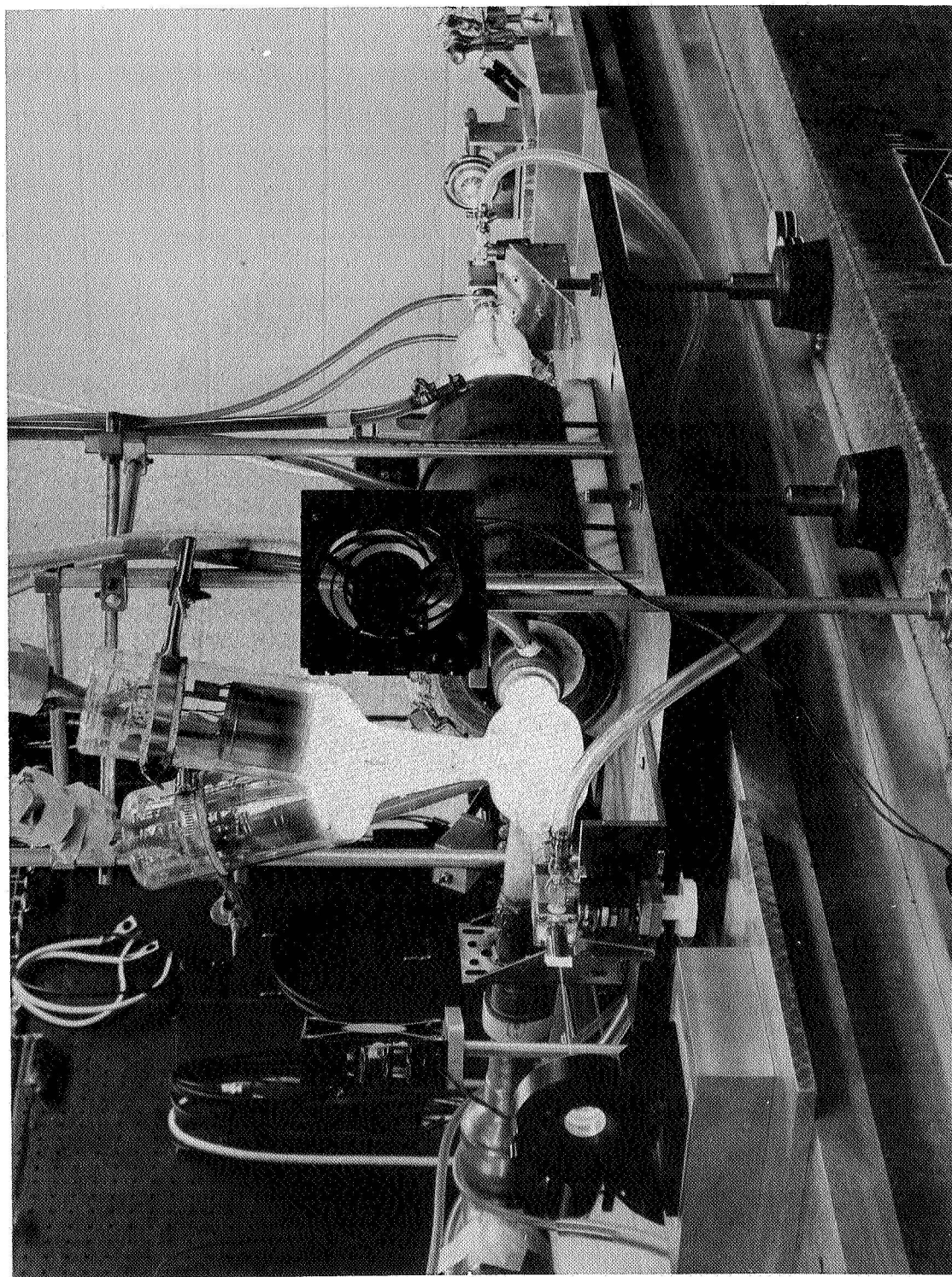
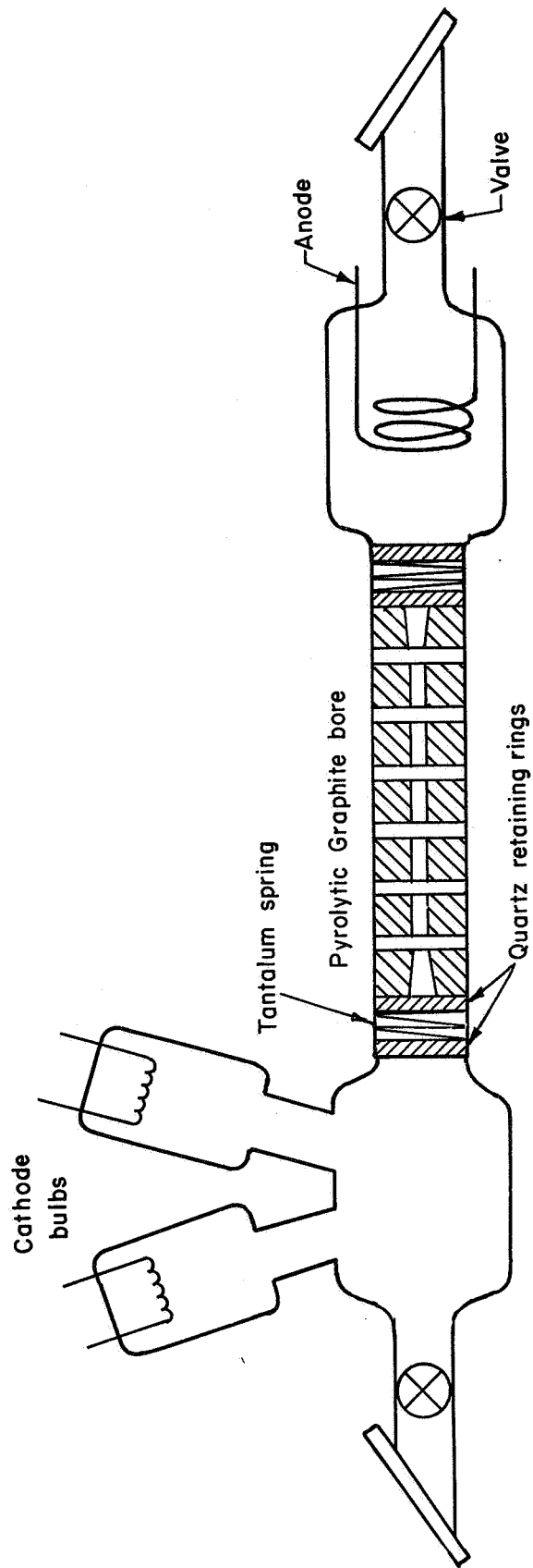


Fig. 8 The Segmented Pyrolytic Graphite Bore Laser



SCHEMATIC DIAGRAM OF PYROLYTIC GRAPHITE BORE LASER .

FIGURE 9

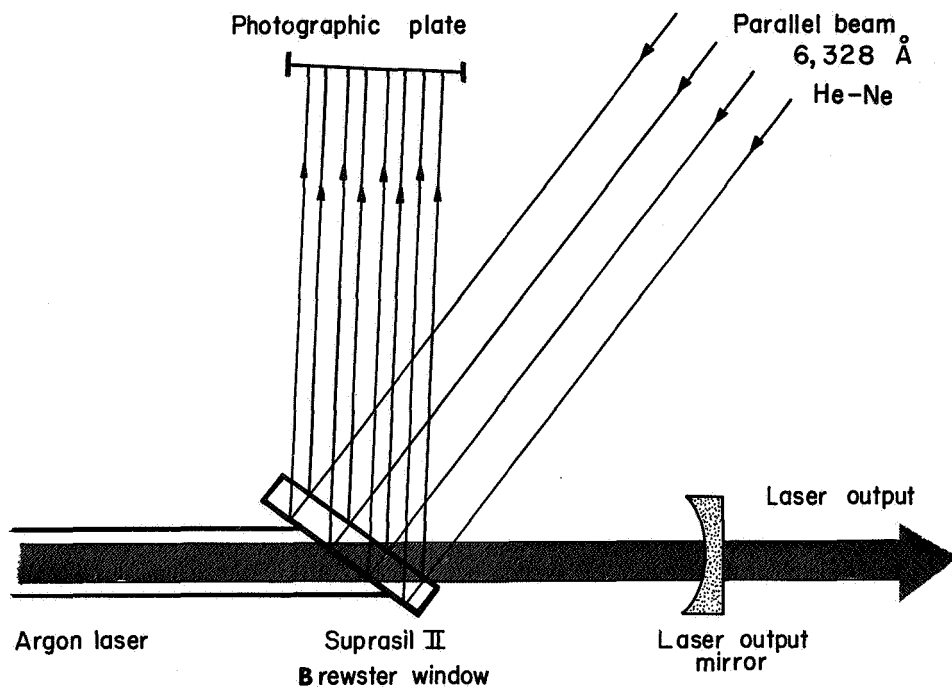
TEST RESULTS

Degradation of the Windows

The Brewster-angle window itself, with its simple geometry and high optical quality, was used to study the nature of the optical degradation occurring during high power lasing. The optical figure of the window was monitored during lasing operation by means of a shearing interferogram produced by light reflected from the two finished surfaces. The experimental arrangement is shown in Fig. 10.

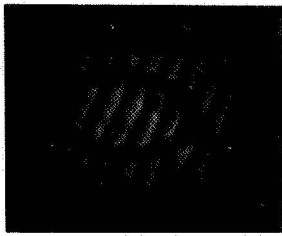
An interference pattern consisting of parallel light and dark bands can be obtained from the reflection of the two flat, but not necessarily parallel window surfaces. Any variation from flatness on one of the window surfaces will appear on the interferogram as a bending of the bands in the area concerned. Interferograms obtained from a window mounted on the principal laser are displayed in Fig. 11. The rectangular flat was mounted on a tube which was cut at Brewster's angle. The contact area when viewed normal to the flat appears as an ellipse about 15 mm by 25 mm. The photograph labeled "Laser Off" in Fig. 11 depicts an interferogram obtained from an undistorted flat; the dark elliptical band marks the contact region. A surface distortion which developed in the first minute of laser operation is clearly visible in the center photograph. After 35 minutes of operation a severe, localized distortion had developed, as indicated by the bottom photograph.

Analysis of the nature and location of the interferogram pattern established that the distortion was a local lenticular deformation of the inner surface of the flat. The output power decay and beam distortion shown in Figs. 1 and 2 were observed to correlate with this deformation of the window. When lasing was interrupted, the deformation relaxed but returned rapidly when the beam was re-established, accompanied by the sequence of changes in the output beam characteristics. However, if the degraded window is removed from the system and reversed, no such rapid power decay occurs; the long-term decay only commences after the fresh surface has been exposed to the discharge for some length of time. Tests were made with windows which previously had both surfaces, in turn, exposed to the discharge. Interferograms showed in each test that only the inside surface exposed to the low pressure discharge environment deformed. At no time was bulk heating of the window observed. Further experiments with a second Brewster window completely inside the vacuum envelope again confirmed the observation that the degradation and associated deformation were localized at or near the surface of that window exposed to the discharge region.

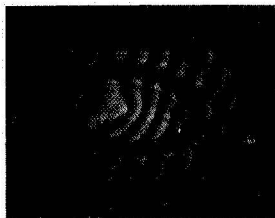


ARRANGEMENT OF APPARATUS FOR OBTAINING SHEARING
INTERFEROGRAMS OF BREWSTER ANGLE WINDOW

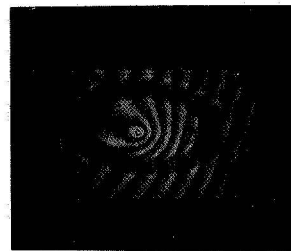
FIGURE 10



Laser off



70 amp discharge 10 watts output after 1 minute



70 amp discharge 5 watts output after 35 minutes

SHEARING INTERFEROGRAMS OF BREWSTER
ANGLE WINDOW DURING LASER OPERATION

FIGURE II

Aging of the Structure

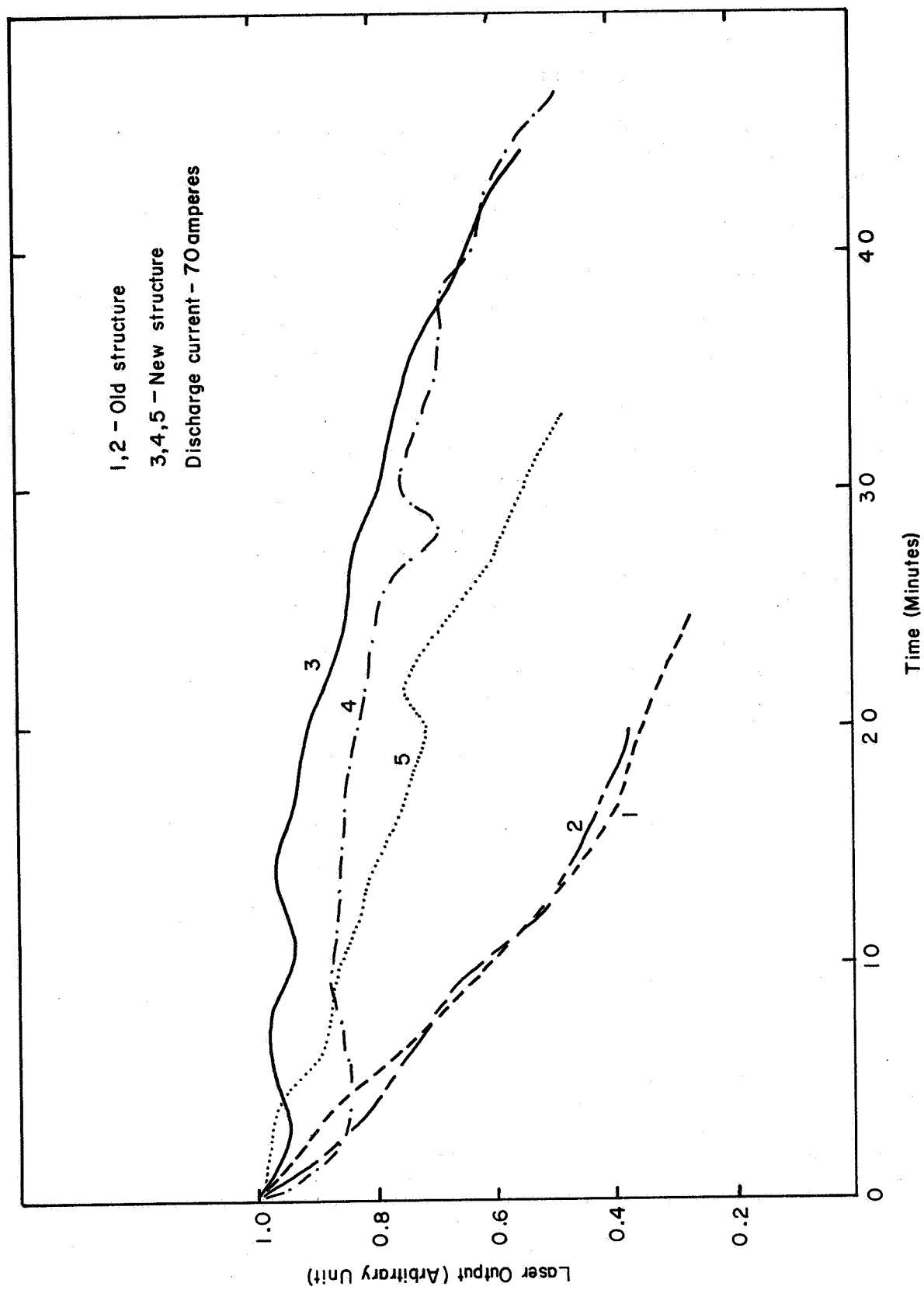
As was mentioned in the Introduction, wide variations in the rate of optical degradation have been noted among various discharge structures. Indeed, a range of power decay rates was observed for the principal laser under identical operating conditions. In particular, the decay rate showed an increase with the age of the discharge structure.

This relationship became evident when the discharge structure of the principal laser was replaced following a break in the bore of the initial structure. A substantial decrease in the decay rate was observed with the new structure, as compared with what had appeared to be the relatively stable rate of the old structure. In Fig. 12 normalized plots obtained with each structure are compared. Run 1 was obtained with the old structure just prior to tube failure, while run 2 was made a year earlier when that structure had been in operation a few months. Curves 3 and 4 represent runs made soon after installation of the new structure, and Curve 5 a run made a few weeks later. The increase in the decay rate of run 5 compared to the earlier runs 3 and 4 represents a structure aging effect which is better shown in Fig. 13. Here runs 1, 3, and 5 of Fig. 12 are replotted and relabeled O, A and B respectively; they are compared with an additional run C obtained six weeks after run B. It appears that the older the discharge tube, the easier it becomes to induce degradation of fresh windows. It should be noted that, during the six-week interval, between runs B and C, many hours of 70 - 100A operation were logged, much in contrast to the history of the earlier structure where such operating levels were quite limited in duration. This, no doubt is related to the reasons why the earlier structure exhibited such an apparently stable and history-independent, damage-inducing capability.

Influence of the Laser Beam on the Rate of Degradation

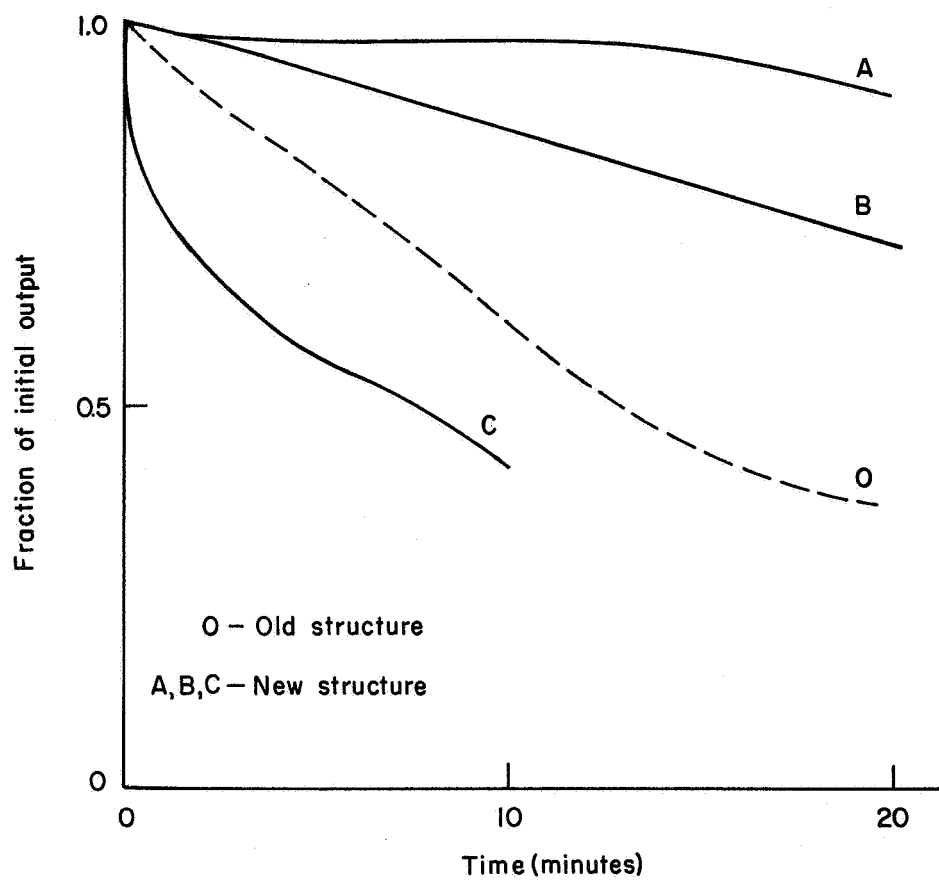
A simple, qualitative test to determine the extent of window degradation with respect to a given operating level of a laser is to observe the beam geometry and power immediately after the onset of oscillation. That portion of the plot in Fig. 7 after the 20-minute mark represents the effect of a badly degraded window on laser output. The time required for the output power to fall from the initial to the final cw value provides a measure of the degree of degradation.

This test was used as a criterion to evaluate the effect of window exposure to the nonlasing discharge. Observations made with a number of windows yielded somewhat inconclusive results. In most cases, at medium and low current, exposure to the discharge only was sufficient to degrade the window to about the same extent as a similar exposure to the discharge and beam simultaneously. However, in a few cases, discharge exposure runs produced little or no effect on the condition of the windows. These tests were performed with the first discharge structure under conditions represented by Curve 1 of Fig. 12. Later, a variation of this procedure was tried with the new structure when the high degradation rate (represented by Curve C of Fig. 13) was occurring. In order to further discriminate between the presence



COMPARISON OF DECAY RATES OF LASER OUTPUT DUE TO WINDOW
DEGRADATION FOR OLD AND NEW DISCHARGE STRUCTURES.

FIGURE 12



CHANGE IN OUTPUT POWER DECAY WITH
USE OF DISCHARGE STRUCTURE

FIGURE 13

or nonpresence of the beam, prior window exposure was made at a higher discharge current (90 A) than that (70 A) used in the earlier tests. Figure 14 shows the relative effects of a seven-minute exposure to a 90 A discharge, lasing and nonlasing, on operation at the 70 A level. In this case there was evidently quite a difference between the lasing and nonlasing situations. The presence of the laser beam seemed to increase the damage rate significantly.

Direct Detection of Optical Damage

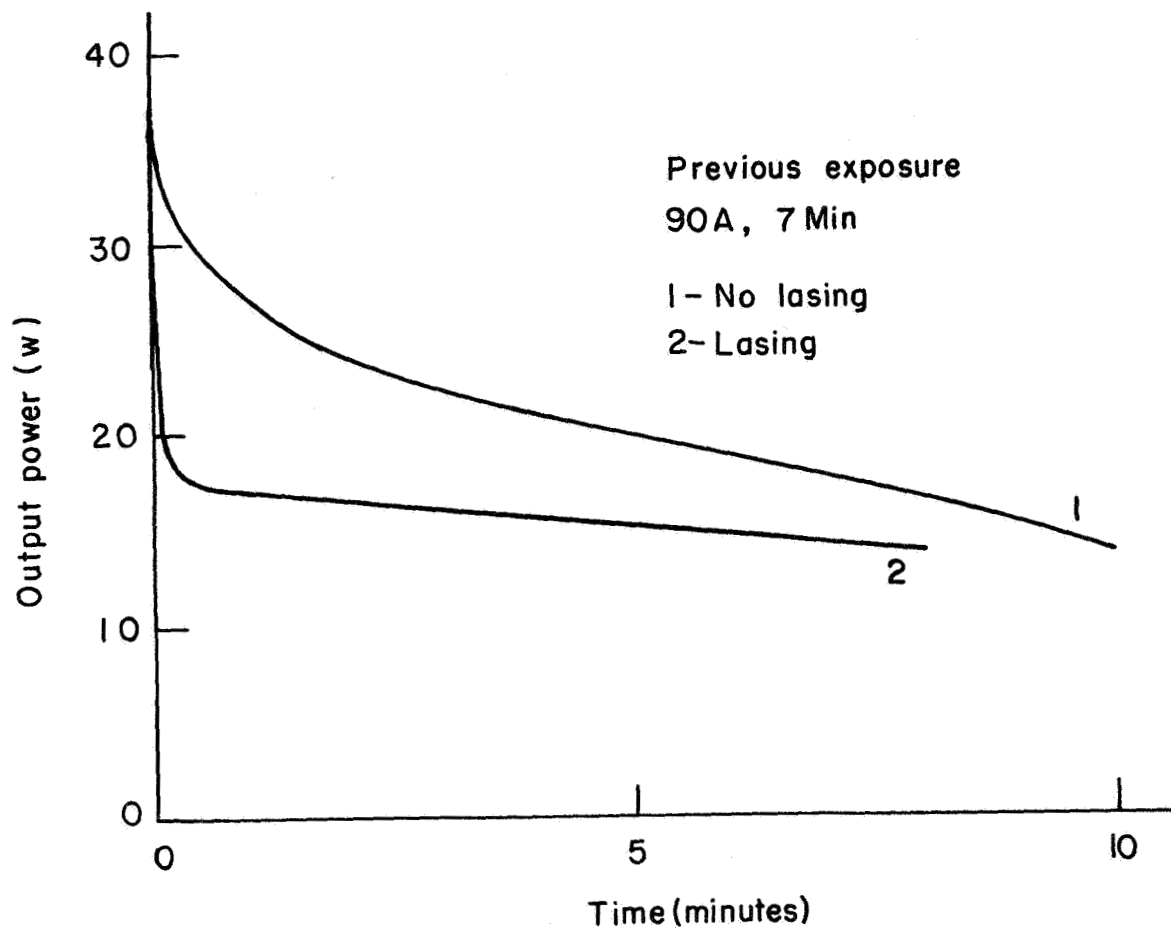
While the effects on laser performance gave clear indication of window degradation, a more direct technique of assessing the damage was desired. Single-pass optical absorption and interferometry were found to be completely inadequate. After some experimentation, two phenomena were found to be effective indicators of surface damage.

Visual inspection of a damaged window through a filter which blocks the scattered lasing radiation reveals an orange-red glow, appearing even before the degradation is noticeable, where the beam impinges on the inner surface. The mode structure of the beam is delineated by intensity variations of this glow. Comparison with a similar fluorescent glow produced by argon laser radiation in glass suggests this is also a fluorescence. This effect has been noted elsewhere.³ The intensity of the fluorescence correlates well with the degree of degradation.

The other technique involved direct visual inspection of a breath-fogged surface. As the condensation begins to evaporate, well-defined patterns emerge. This differential rate of evaporation on the exposed surface is probably a result of variation in the surface thermal conductivity associated with film formation or local alteration in the surface structure. The "breath test" proved to be a simple criterion of window degradation and was particularly useful for assessing the effectiveness of different cleaning or window restoration techniques. An example of such a circular condensation pattern on an exposed mirror is shown in Fig. 15. Similar elliptic patterns were observed on Brewster windows but because of the very low contrast were difficult to photograph adequately.

Cathode vs Anode

As there had been some previous experiences which suggested an asymmetry in the damage rates between the anode and cathode windows, several experiments were carried out on the graphite laser using Brewster windows on both ends. With a seven percent transmission output mirror, an initial output power value of 3.5 W was observed with a 40 A discharge current. This initial power density of 700 W/cm² was sufficient to produce thermal distortion should an absorbing surface film form. The fluorescent glow appeared on both windows within the first minute of lasing.



OUTPUT POWER DECAY USING WINDOWS PREVIOUSLY EXPOSED TO
LASING AND NONLASING DISCHARGE

FIGURE 14

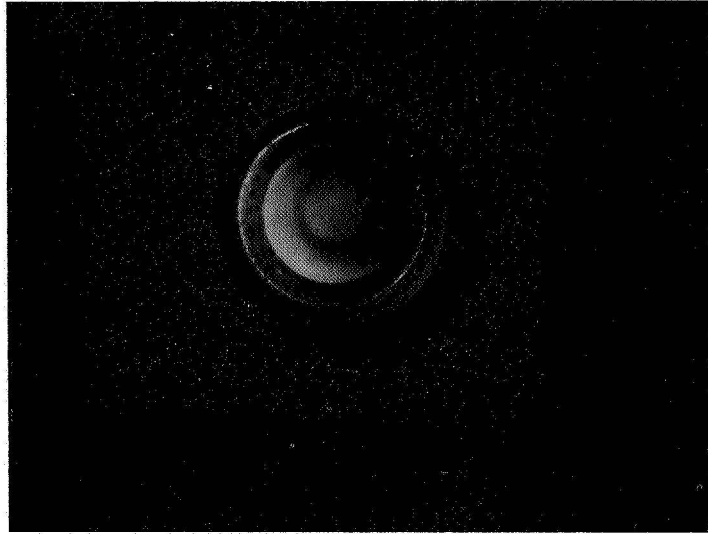


Fig. 15 Fog Pattern Produced on Cooled Mirror
Surface After Exposure to Lasing Discharge

Shearing interferograms revealed a distortion of the window at the anode end after ten minutes. Slight distortion of the cathode window was noted after 30 minutes. The output power dropped to half its initial value after 120 minutes, at which time the distortion of the anode window was much more severe than that of the cathode window. Runs were made, using fresh windows each time, with only one cathode operating and with both cathodes running at a lowered temperature; the results were identical to those of the initial run.

Window Mounting and Cleaning Procedures

Throughout the first half of the program the Brewster-angle windows were mounted by affixing an optical flat to a properly cut and ground section of tubing using a low vapor-pressure vacuum grease. During this time some of our flats were sent to a vendor to be fused to suitably cut quartz tubing. After some unsuccessful attempts, fused-on window structures became available for testing. Tests run on the anode end of the structure yielded surprising results. Little or no fluorescence was found at lower power (70 A, 40 W) and it completely disappeared during higher power operation (80 - 90 A, 60 - 75 W). Subsequent operation at all power levels showed no window deterioration on the time scale to which we had become accustomed.

An inquiry was made to the vendor who fabricated the fused-on mounts as to the cleaning procedure used. The vendor cleans the windows with solvents and chromic acid glass-cleaning solution before mounting. After mounting, the structure is dipped in the acid solution, rinsed with distilled water and then annealed in air at 1100°C for several hours. There was no further cleaning of the inner surface by the vendor or this laboratory.

In view of the above results, tests were run on windows mounted in the laboratory using a low vapor pressure epoxy in place of the vacuum grease. Coincidentally, at that time a different cleaning technique was used. The procedure for preparing and mounting started with cleaning the window by dipping it in hot glass cleaning solution followed by 15 to 30 minute immersion in a strong detergent solution. The cleaned window was rinsed with distilled water, air dried and then coated with collodion. The dried collodion film was removed just prior to mounting the window. The window was mounted by means of epoxy on a similarly cleaned quartz tube, which had a suitably polished Brewster-angle cut.

Windows which were so prepared and mounted also displayed no symptoms of film formation. One of these logged a total of 58 minutes of operation with a 90 A discharge and 75 W output (7 percent transmission).

Subsequent testing determined that the presence of vacuum grease (Apiezon H) on the window results in rapid optical degradation. A window

which had been cleaned following the above procedure was mounted using vacuum grease. With a 70 A discharge a decline in power output to half its initial value, accompanied by mode instability, occurred in 15 minutes. The effects of grease were tested also with one of the windows mounted with epoxy. After successful operation at 80 A for 35 minutes, some grease was applied to the inner surface at the periphery. Subsequent operation at 80 A gave a 60 percent drop in output power, accompanied by mode instability, in 12 minutes. At no time during these tests did the lasing beam impinge on the grease.

While the freshly cleaned windows, either fused or epoxied, appeared to be damage resistant, several incidents pointed to a restricted shelf life. For one particular case, a fused-on window, when initially received, exhibited no deformation at sustained high output power levels (65 W). The window was retested after being "on the shelf" for two weeks. While on the shelf the window mounting tube was sealed so that the inner window surface was kept free of dust and other contaminants. The window exhibited immediate distortion with a 60 A discharge. The output power at this current was 20 W. The distortion was so severe at 70 A that the output power was limited to 15 W. This effect was observed several times and is not really understood as yet.

Discharge Structure Erosion

Principal Laser

Two catastrophic failures of the principal laser occurred during the course of this study. The first of these resulted from a clean break of the bore approximately one-third of the distance from the anode end. Examination of the fracture site revealed no serious erosion or burning of the quartz. The failure occurred during high current operation (120 A) and apparently resulted from some local strain condition. A replacement discharge tube failed when a break occurred at the ring seal joining the bore to the tapered section at the cathode end and most probably was due to improper circulation of the coolant at that point.

Inspection of the broken capillaries revealed darkened areas at various places. Microscopic examination of these areas showed that the quartz was badly eroded. The brownish color was found where the quartz seemed to have melted and resolidified. The discoloration was not on the surface but rather permeated glassy nodules and ridges on the quartz. The most severe bore erosion occurred adjacent to the tapered section. Here there was a spiral formation of alternating clear and dark bands; a scalloped erosion formed the clear regions, while the dark bands were made up of the discolored glassy nodules and ridges. A thick deposit of similar dark material was found on

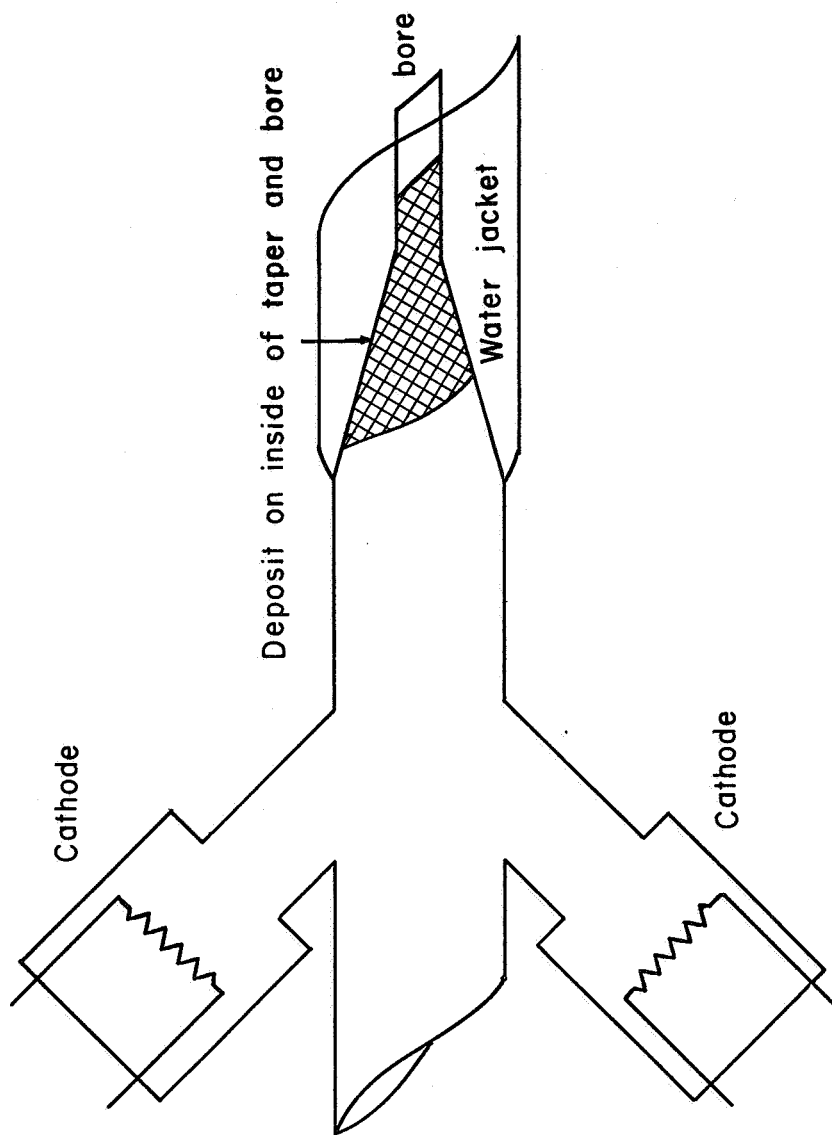
the tapered section at the cathode end, as indicated in Fig. 16. The location and thickness of this deposit relative to local irregularities in the tube diameter indicate that material emanating from the bore had deposited in this relatively cool region.

Various techniques were employed to determine the composition of the deposit. Chemical analysis of scrapings taken from the area indicated the material to be mostly SiO. X-ray powder patterns show that there is some ordered structure in this material but complete identification was not determined. X-ray microprobing with a 1μ diameter beam indicated the presence of silicon and argon. Oxygen did not register, as this particular instrument was restricted to elements heavier than sodium. The microprobe showed also that the argon was limited to the deposit, for none was found in the underlying quartz. This is possibly due to the fact that argon bombardment of the bore is an important part of the erosion process; or perhaps argon ions are driven into the deposit as it forms since the magnetic field lines at this point run parallel to the bore and thus impinge on the surface of the taper.

When the principal laser was restored to regular operation by the installation of a new discharge tube some unusual effects were observed. After approximately one hour total running time at discharge currents of 70 to 90 A, the characteristic spiral bore erosion pattern became evident at the throat of the cathode taper. Black wall deposits from the cathodes were observed to migrate along the walls of the cathode bulb necks onto the tube wall at the entrance to the taper. After several hours of operation these black deposits cleared up. A pronounced sodium glow at the base of the cathode bulb was observed during initial operation of the discharge. This glow results from sodium impurities in the BaSrO₃ cathode coating. Of more interest is the fact that when the discharge was first brought up to about 50 A a sodium glow was observed in the anode bulb and persisted on the wall at the neck of the anode bulb. Obviously, the discharge is capable of pumping metallic constituents of the cathode structure to the anode end of the tube, 2.5 meters away.

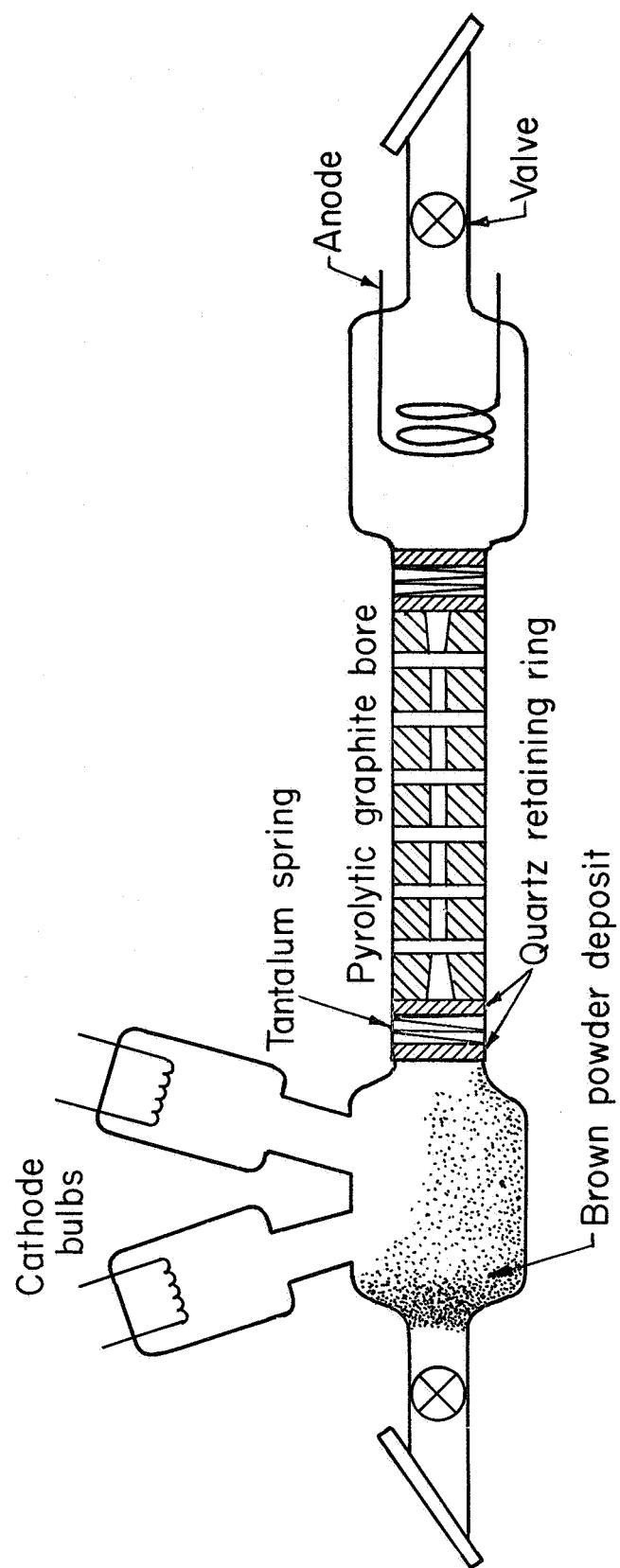
Graphite Laser

A brownish deposit accumulated on the walls of the bulbous section at the cathode end of the pyrolytic graphite bore laser as indicated in Fig. 17. When a modification of the structure was made, this material was removed and proved to be powdery in composition. This powder deposit had slowly accumulated during the previous eight months of laser operation. Samples of this powder were analyzed with the electron beam microprobe. The analysis revealed that some particles showed only the presence of silicon, while others contained no silicon but instead many other metallic elements. Listed in order of decreasing amounts, these elements were: Ba, Fe, Mn,



LOCATION OF DEPOSIT AT CATHODE
END OF DISCHARGE TUBE

FIGURE 16



SCHEMATIC DIAGRAM OF PYROLYTIC GRAPHITE BORE LASER

FIGURE 17

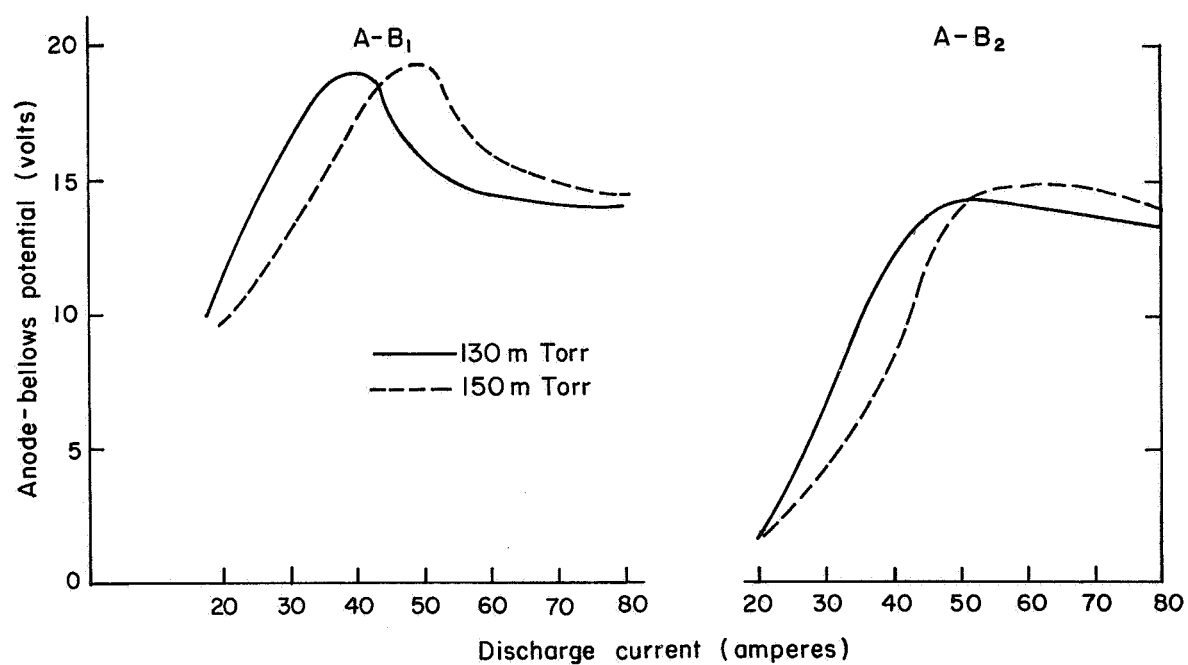
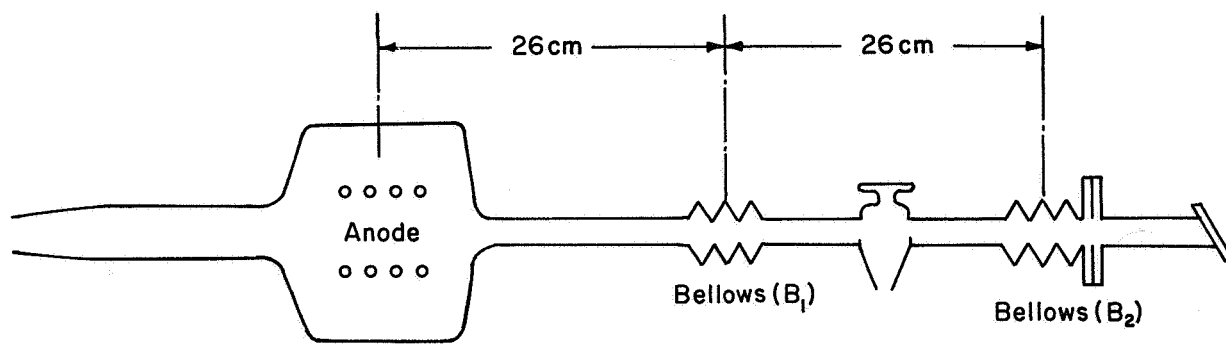
Ni, Cr, Sr (trace). It would seem that the powder is made up of a mixture of material from the cathode structure and eroded material from the quartz retaining rings which are located just beyond the ends of the solenoid magnet.

Transport Studies

In order to gain insight into possible transport mechanisms for film-forming particles, measurements were made of the electrical potential in the region between the electrodes and the terminal optics. A suitable high impedance voltmeter was used for this purpose. Metal bellows which are located in this portion of the envelope were used as measuring points. Figures 18 and 19 list in graphic form the potential variation with discharge current at the test points for two different fill pressures. Note that in Fig. 18 the anode is positive with respect to the bellows while in Fig. 19 the cathode is negative with respect to the bellows. Examination of this data indicates that, as the current is increased, a gradient is established to compensate for those particles accelerated past the electrodes. However, as the discharge current is further increased, the conductivity of the plasma in the region increases until a current-free gradient can no longer be sustained.

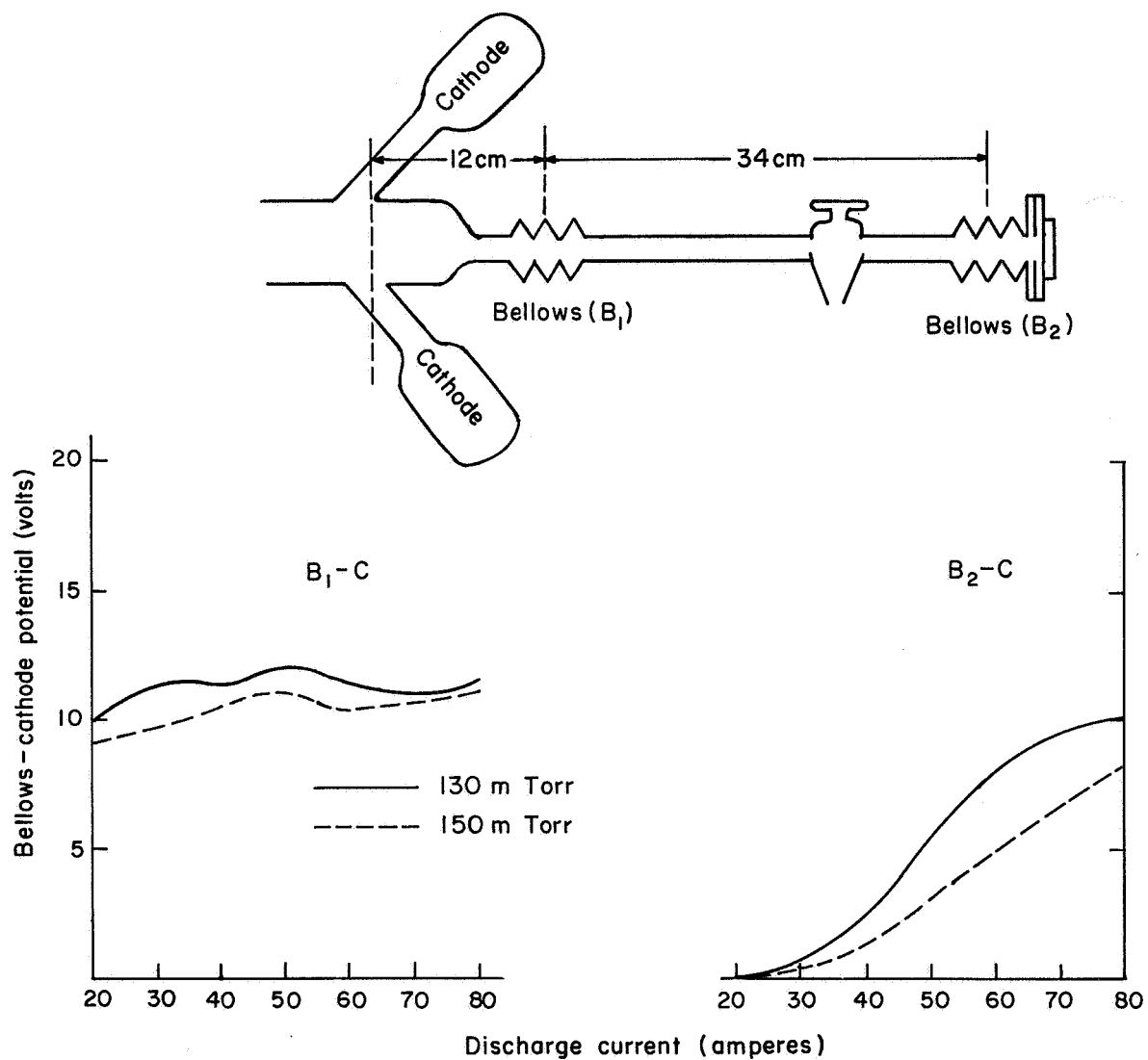
If a potential gradient between the anode and the end bellows was artificially introduced by establishing a current-limited ground path, as indicated in Fig. 20, the resulting field was sufficient to transport negatively charged particles toward the anode. Some particles, believed to be grease particles emanating from the stopcock, scattered the lasing radiation and thus acted as tracers of this charge transport. These particles were constrained to move down the center line of the envelope by the repulsion of the static negative charge on the walls. That they were negatively charged was confirmed by magnetic deflection of the stream of particles. Near the anode bulb a cusp-shaped distribution of suspended particles was observed which presumably marked the juncture with the electron stream accelerated through the anode. This cusp-shaped distribution of particles moved further away from the anode with increasing discharge current. When the ground path was removed from the bellows, the larger particles immediately dropped to the bottom of the tube and the smaller particles rapidly moved away from the anode, decelerated and gradually diffused out of the beam.

This particle transport is shown in the photos in Fig. 21 which view the section of the envelope between the anode bulb and the first bellows (B_1). In Fig. 21b the confined stream of particles and the terminating cusp formation are visible. The initial dispersal of the particles after removal of the ground connection is pictured in Fig. 21c. Similar particle behavior was noted at the cathode end of the structure when a potential of 200 V was established between the two bellows sections.



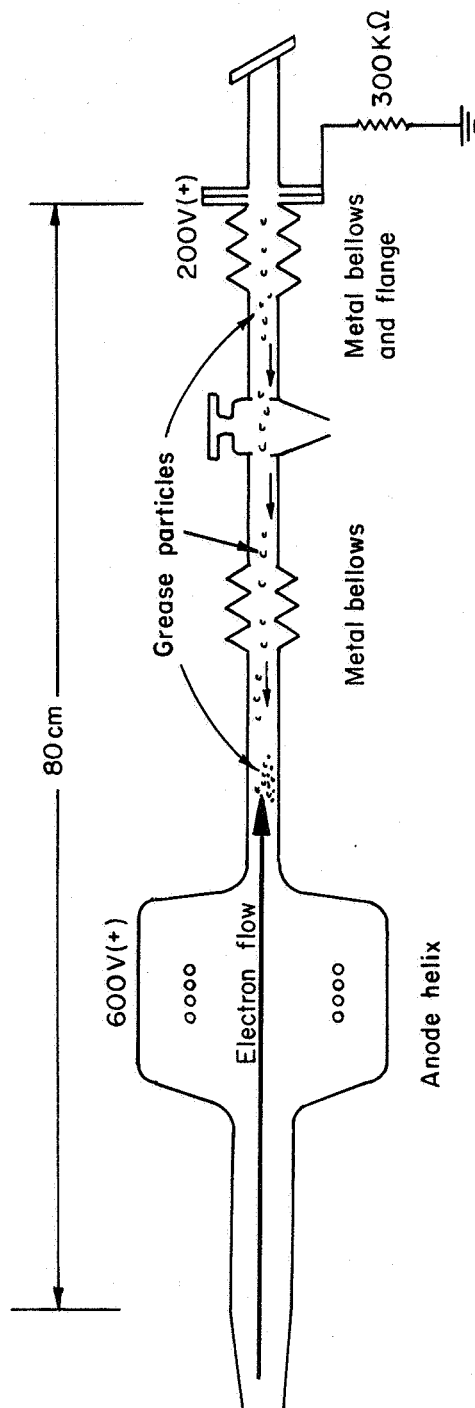
POTENTIAL GRADIENT IN PLASMA REGION BEYOND ANODE VS DISCHARGE CURRENT
(PRINCIPAL LASER)

FIGURE 18



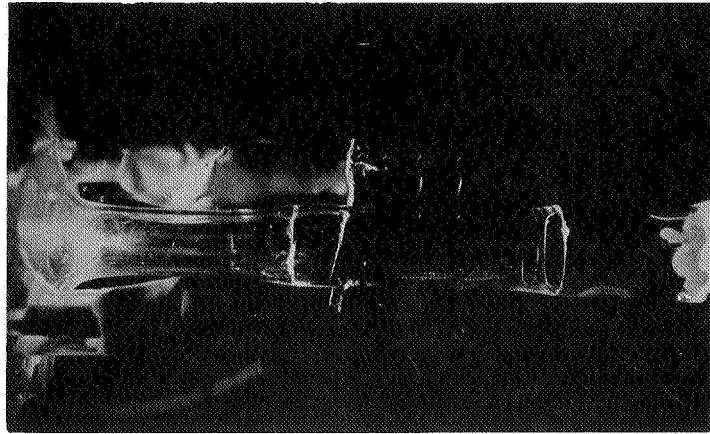
POTENTIAL GRADIENT IN PLASMA REGION BEYOND CATHODES vs DISCHARGE CURRENT
(PRINCIPAL LASER)

FIGURE 19

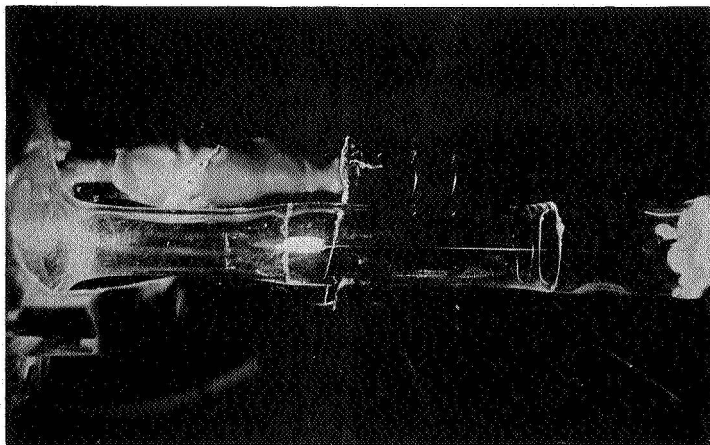


PARTICLE FLOW OBSERVED WITH VOLTAGE GRADIENT ESTABLISHED
BETWEEN END FLANGE AND ANODE

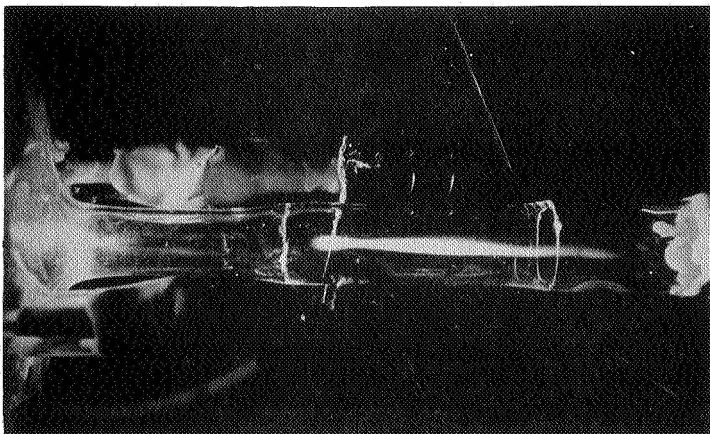
FIGURE 20



a) No potential gradient



b) Gradient established: Particle streaming



c) Gradient removed: Particle dispersal

Fig. 21 Particle Transport in the Region between the Anode and the End Bellows: Anode-Bellows Potential Difference 600V

It is clear that, at high current levels, charged particles are accelerated for some distance beyond the electrodes. An instance of gross particle transport was noted here recently when particles ejected from a graphite bore during high current operation were deposited on the end window, which was some 40 cm beyond the anode. In this case the graphite particle movement was opposite to that of the gas circulation.

Counter Measures

Heating

The fused quartz window mounts were used to test the effect of heat on the film deposit. In the initial attempt a method was devised which provided for heating the window during lasing operation. A heating wire and thermocouple were fixed to the window with epoxy. In order to eliminate optical distortion of the cavity due to heating of the surrounding air, as well as to limit the heat loss, the heated window was enclosed in an evacuated chamber terminated by a mirror. A viewing port was provided to obtain shearing interferograms.

Temperatures up to 400°C were attained with this arrangement and the observation of the interferograms indicated the window was heated uniformly. Observation of the window while lasing with a 70 A discharge indicated no reduction in the window degradation rate. Indeed, there was some evidence that the heating enhanced the degradation.

In subsequent tests an oven was placed around the window so that higher annealing temperatures could be obtained. The window used had experienced severe film deposition and exhibited the usual symptoms of fluorescence, beam distortion and power limitation. With a 70 A discharge current the output power was 15 W (7 percent transmission).

The window was subjected first to a baking cycle with the discharge tube evacuated. Extreme distortion which limited the output to 3 W with a 60 A discharge was observed after baking at 470°C for 30 minutes and 650°C for 30 minutes. Utilizing the three-way stopcock, air was let into the window mounting tube while the rest of the discharge structure was kept evacuated and the window was baked for one hour at 750°C. Much improved performance was noted following this air bake. Although the fluorescence was noted, an output power of 35 W was obtained with a 70 A discharge. A similar baking run using oxygen-enriched air improved the performance slightly.

Sputtering

Following the baking tests, the window was subjected to argon sputtering using 16 Mc rf, 2.5 kV peak to peak. The argon pressure was 15 m torr. The rf field was produced between an aluminum foil electrode pressed against the window and the mounting flange of the window support tube. Little change in the lasing characteristics was noted after sputterings of 5 and 20 min. duration, although all fluorescence and scatter disappeared from the inner surface after the 5-min. application.

The window was next sputtered for 30 min. with oxygen. The window was found to be optically degraded with fluorescence again observed on the inner surface. The lasing performance was:

60 A - 25 W - dropped to 15 W in 6 min.

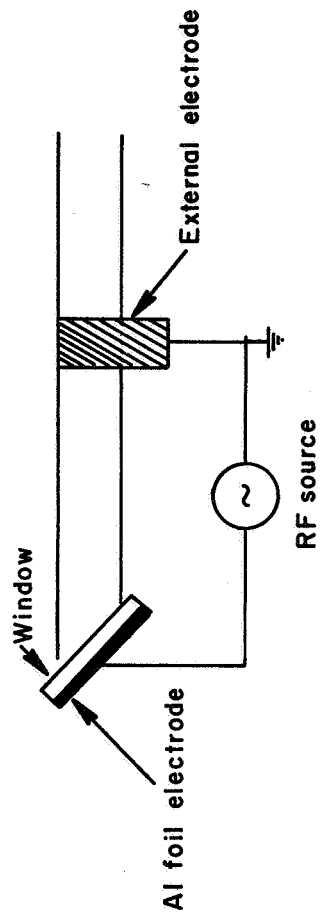
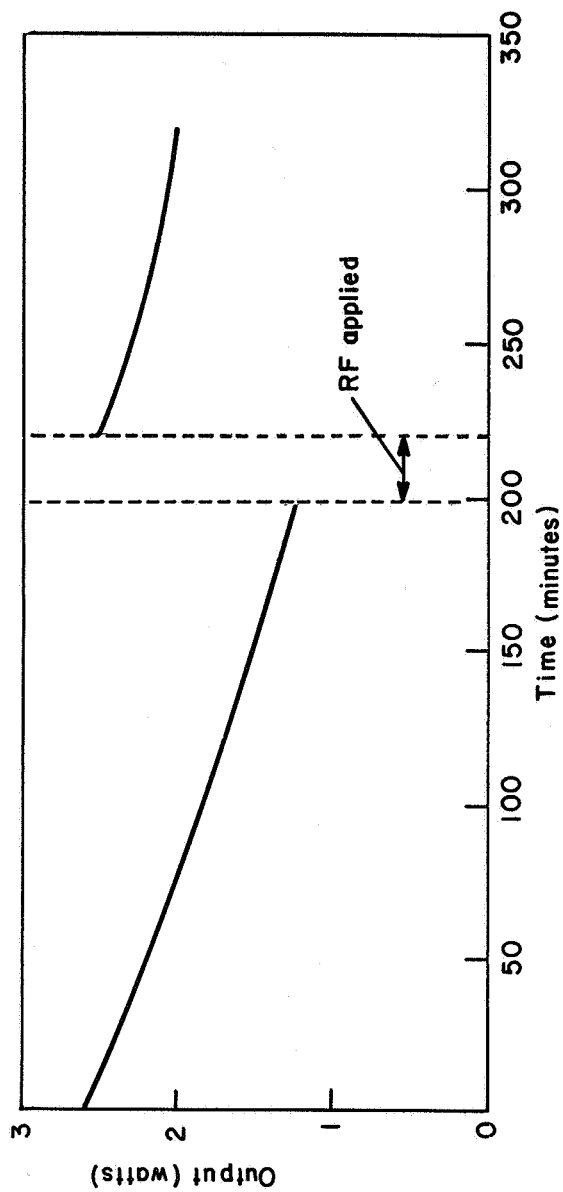
80 A - 20 W - dropped immediately to 15 W, complete distortion of beam.

A subsequent 5-min. sputtering with argon removed the fluorescence but window distortion still occurred at 80 A. However, following a 30-min. argon sputtering the window was restored to the condition which existed prior to the oxygen sputtering. A 30-min. oxygen bake had no further effect.

In further tests, film removal by argon sputtering proved to be quite effective even with normal gas fill pressures. Degraded windows located at either the cathode or anode end of the laser structure were restored by this means. These results were obtained for the pyrolytic graphite bore laser (Fig. 22) as well as the principal laser. Later it was determined that the sputtering could be accomplished using a Tesla coil as the rf source. Although the windows were restored to their original condition by the sputtering action, renewed film deposition commenced soon after the sputtering ceased. Additional tests with Tesla coil applications of the rf to the region of the mounting tube away from the window while the laser was operating showed that, not only was film removal accomplished, but also that film regrowth was somewhat inhibited.

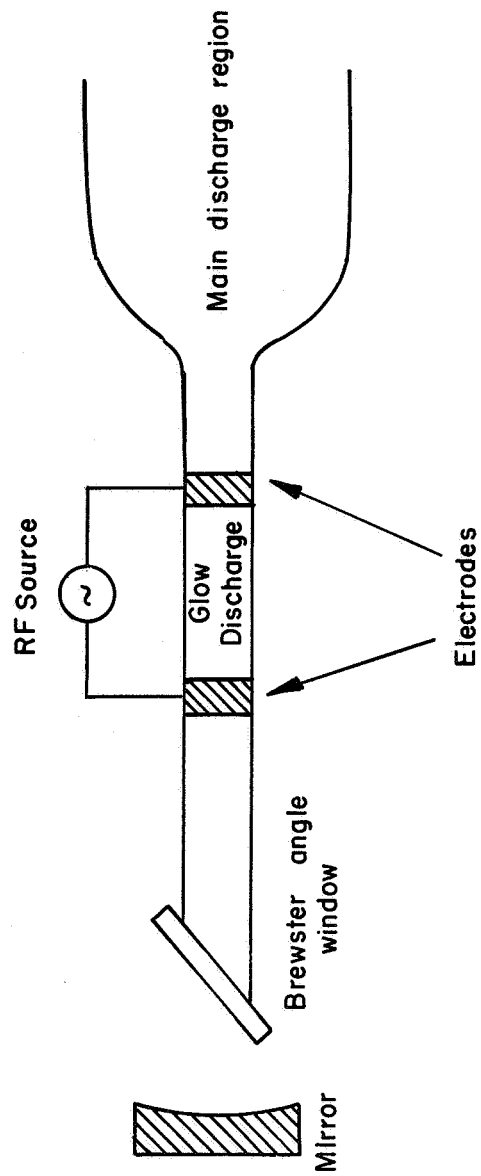
This result was followed up using a more refined method establishing the rf discharge, in which the rf was applied between an external electrode around the tube, located a few centimeters from the window, and the flange while the laser was operating as is shown in Fig. 23. A dramatic cleanup of the window (Fig. 24) was observed within the first minute after initiating the rf discharge. Further tests with the rf technique, which had no adverse effects on the output during the application time, indicated that re-establishment of the window film was inhibited particularly with high discharge current and high optical power operation.

The establishment of a dc glow discharge, regardless of polarity, in the region between the window and the laser electrode had no noticeable effect on window degradation.



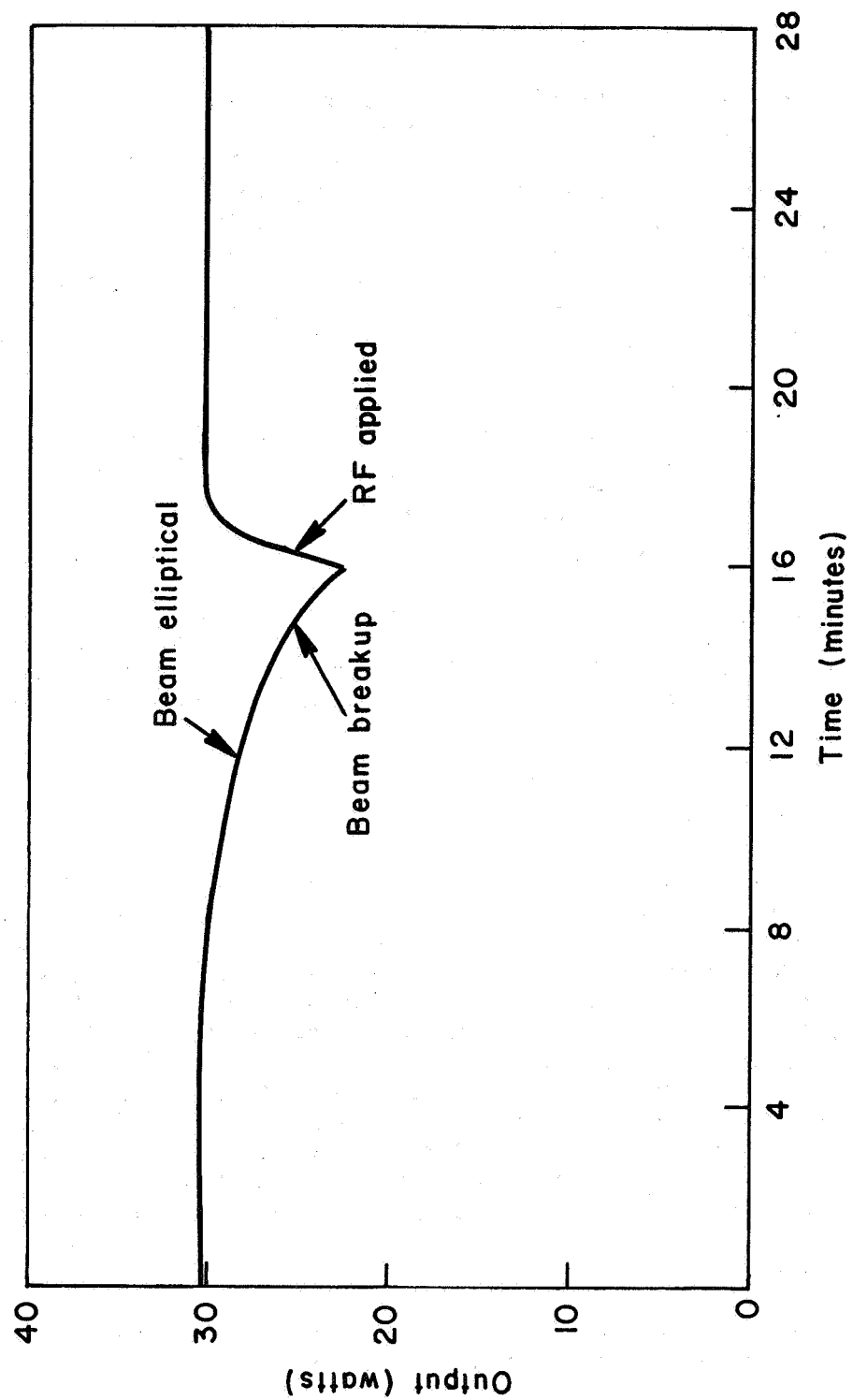
EFFECT OF ARGON SPUTTERING OF DEGRADED WINDOW ON OUTPUT
(PYROLYTIC GRAPHITE BORE LASER; ARGON PRESSURE 450 MTORR)

FIGURE 22



RF DISCHARGE USED FOR THE RESTORATION OF TERMINAL OPTICS

FIGURE 23



EFFECT OF RF DISCHARGE ON OUTPUT (PRINCIPAL LASER)

FIGURE 24

Mirror Heating

A study was made of the effects of thermal distortion of the mirrors on the performance of the laser. The use of various output couplings to control the loading on the mirrors led to the observation of significant thermal effects. Output coupling values of 34 and 24 percent were tested using 10-meter radius substrates which were only 0.75 in. dia. by 0.25 in. thick. This configuration was much more sensitive to heating than the larger, shorter radius standard geometry. The results of the experiments with the 24 percent output coupling are given in Fig. 25. Rather large temperature rises were observed on both mirrors. With severe heating the laser output power fell about 10 percent.

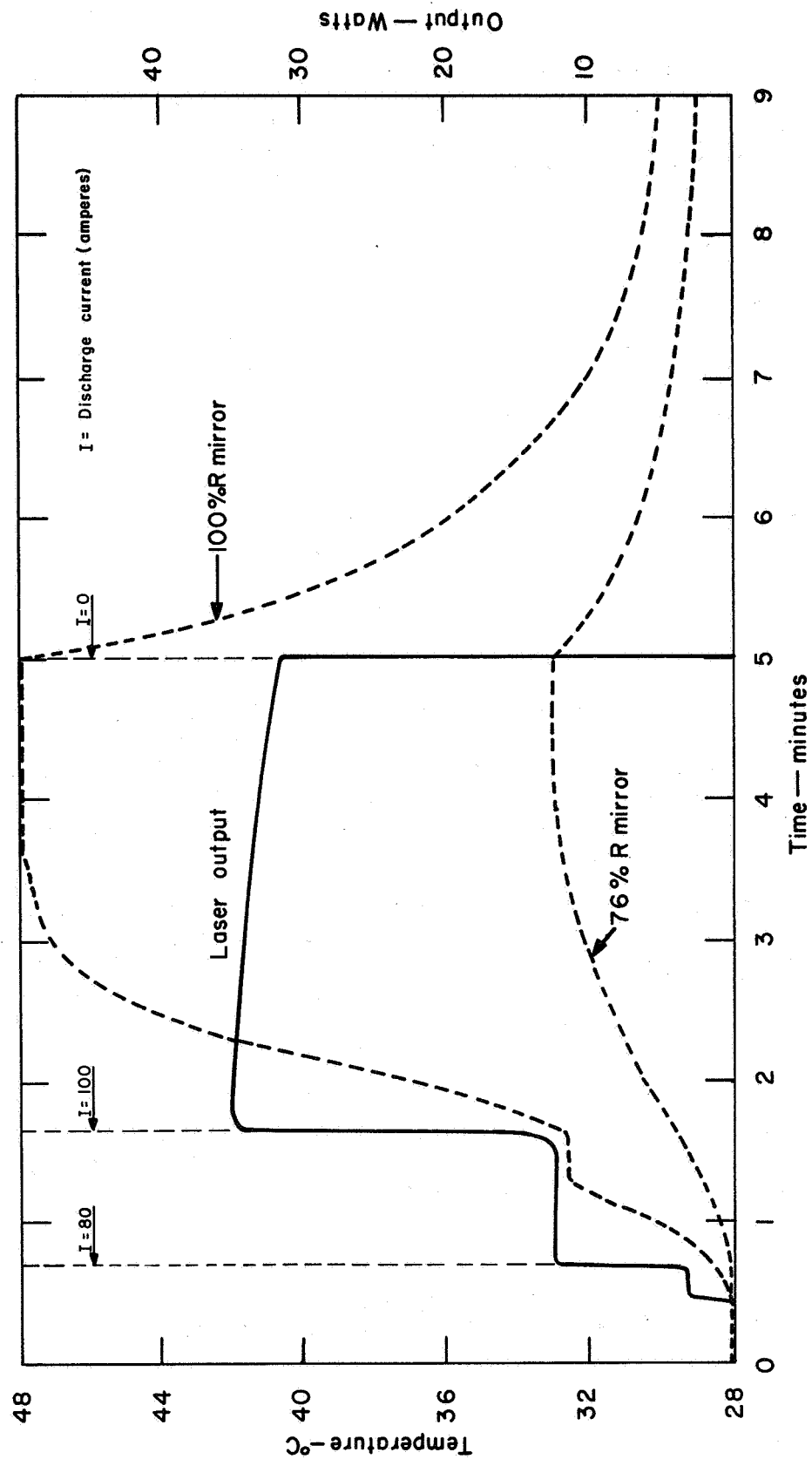
The absorption of this much heat in a Brewster window would probably reduce the laser output to almost nothing. The mirrors are clearly less sensitive to thermal distortion effects and the best laser performance for extended periods was always obtained with directly mounted internal mirrors rather than with Brewster windows.

The "breath test" revealed a changed surface condition over the circular area exposed to the discharge on many of the mirrors after high discharge current operation. On some of these mirrors a second circular area corresponding to the beam size was readily discernible within the larger circle.

Evaluation of Available Commercial Mirrors

During this investigation a program of testing available dielectric-coated mirrors at high power levels was completed. We have investigated the effects of high-power laser operation on mirrors mounted so as to be exposed to the discharge environment as well as mirrors placed external to end windows. In this effort we received excellent cooperation from seven leading vendors, five of whom are located in the Northeast and two on the West Coast. Identically finished, 12-foot radius, 1-1/4 in. dia. quartz substrates were furnished to the vendors for coating. All test sets consisted of a maximum reflectivity mirror covering all argon wavelengths, and a 16 percent transmission mirror centered at 5000 Å. In most cases best-effort coating procedures were employed, at no charge. These test coatings were compared in terms of surface scatter, power achieved with comparable discharge conditions, heating during high power operation and resistance to bleaching or cracking.

Table I shows the output power from each set of coatings at the start of each test. These mirrors were O-ring mounted on the principal laser.



BULK TEMPERATURE OF END MIRRORS MONITORED DURING LASER OPERATION.

FIGURE 25

Table I
Maximum Power* Output in Watts

<u>Vendor</u>	<u>70 amp</u>	<u>80 amp</u>	<u>Input 90 amp</u>
A	34	43	56
B	--	34	51
C	--	--	48
D	42	54	71
E	39	46	62
F	37	40	57
G	38	47	62

* Power as read on a commercial power meter.

Notes on Tests

Vendor A

These coatings showed some scatter loss. During each 15-min. laser run, there was a reversible drop in power due to substrate heating from absorption loss in the coatings. There was some beam shrinkage during the run. The test set was run at 80 A for one hour and at 90 A for one hour with no sign of power loss due to coating damage. Inspection of the mirrors showed no signs of physical damage.

The 100 percent mirror was then run with a 7 percent transmitting mirror to study the effects of higher power densities on the coatings. The output with this coupling was 43 W - 70 A, 56 W - 80 A, and 65 W - 90 A. There was no sign of coating damage; however, there was extreme beam shrinkage at 90 A, and the mirror became quite hot.

Vendor B

These coatings showed some scatter loss. The set was run for one hour at 90 A. There was a definite 15 percent loss of power at the end of the run. The mirrors grew warm during the test.

Vendor C

These coatings showed extremely high scatter loss, the surface looked rough in ordinary light. The 100 percent mirror leaked 5145 A

badly, so readings of power were taken from both ends during the test and added to give a total power output. After running one hour at 90 A, there was a 10 percent decrease in output power. The mirrors ran hot during the test.

Vendor D

These coatings showed no scatter at all. There was no indication of absorption loss indicated by mirror heating. The output power was the greatest achieved in this test. The coatings were run 30 min. at 80 A and 30 min. at 90 A. There was a six percent drop in power after the 90 A run. This was probably due to the same effect that causes window damage and shows on these coatings because they have such a low loss to start with.

The 100 percent mirror was run with seven percent output coupling producing 42 W - 70 A, 57 W - 80 A, and 82 W - 90 A. There was no sign of beam shrinkage, and there was no evidence of a bleach spot or other coating damage after this test.

Vendor E

These coatings showed some scatter loss and slight absorption loss causing minor mirror heating during the run. The coatings were run 38 min. at 80 A and 34 min. at 90 A with no signs of power drop after the test.

When the 100 percent mirror was run with seven percent coupling, the output was 50 W at 80 A. At 90 A the beam shrinkage (due to heating) was so severe that power readings were inadvisable. There were no signs of bleach spot or other physical damage after the test.

Vendor F

These coatings showed a great deal of fine scatter but little absorption. They were run for one hour at 90 A with no sign of power loss. When the 100 percent mirror was run with the seven percent transmission mirror, there was immediate indications of coating damage. Inspection of the 100 percent mirror showed a large, quite visible, bleach spot and the coating was badly crazed.

Vendor G

These coatings showed some scatter. The coatings were run 1 hour and 40 min. at 80 A. There was no sign of power loss; however, a spot began to form on the 100 percent mirror. The mirrors were then run at 90 A for 30 min.; the spot grew to $\frac{3}{4}$ of the mode size. At the end of the test the output power did not seem to have changed much. The spot on the 100 percent

mirror was clearly visible through a yellow filter when the laser was running. When the mirror was removed, a bleach spot could be clearly seen when the mirror was viewed against a yellow background. The bleach spot was almost invisible in ordinary light.

The test results given above were reported to each participating vendor without identifying competitors. The majority of the coatings studied gave comparable results as to output power and beam geometry. The major problem noted was heating at high power levels followed by a deterioration of the coating in the form of bleaching. There seemed to be some correlation between the degree of inherent scatter and the absorption. Heating was particularly severe for those mirrors. It appears that significant reduction in the inherent absorption of coatings must be achieved if very high power (i. e. , 30 to 100 watts), single radial mode output is to be achieved.

DISCUSSION AND CONCLUSIONS

The objective of the present program has been to assess the optical cavity limitations which might be present due to the very high power densities generated in the argon ion lasers. A peculiar progressive degradation of output performance had been noticed at our laboratory several years ago¹ when laser structures capable of twenty watts or more of cw power were first constructed. It was soon realized that this was in some manner associated with the optical loading of the windows and mirrors but the detailed mechanisms were not clear at that time. Since then, the existence of a severe "window problem" has been confirmed by many workers in the field of ion laser technology.

The present contract program was initiated with the primary goal of identifying and, if possible, controlling the mechanisms responsible for the apparent damage to the optical components. Because the problems were very much more severe when Brewster windows were employed than when the mirrors were mounted directly to the discharge structure, the Brewster window was chosen as the focal point of the investigation.

At the onset we considered three likely sources of window degradation: 1) Direct nonlinear effects due to the high power optical fluxes, i. e. , Raman effect, multiphoton processes, etc. , 2) Surface or bulk damage of the window by the ultraviolet generated by the discharge, and 3) The deposition on the window of materials released within the discharge structure from the electrodes on the walls by the erosive action of the high current discharges required for ion laser action. Much of the experimentation reported above was designed to assess the relative importance of these three possible mechanisms. When the dominant process was finally identified as the deposition of contaminants, most of the remaining effort went into clarifying the details of the deposition process and assessing various countermeasure techniques.

The direct nonlinear processes were readily disqualified as the dominant mechanism by the evident time dependence of the observed degradation effects. This clearly implies a process of gradual alteration of the optical components which is not consistent with the concept of a direct nonlinear interaction between the optics and the high photon fluxes. The limitation of such effects should be felt immediately if they are present. In addition, simple numerical estimates show that such effects are not really to be expected at the optical power levels currently obtainable. Some day we may have to face these limitations in ion lasers; however, there are simple, more pressing problems to be overcome first. The problem was therefore quickly reduced to ultraviolet or film deposition, or perhaps some as yet unknown mechanisms.

Untangling ultraviolet effects from the possibility of film deposition proved to be a much more difficult task than originally envisioned. Many of the experiments were quite inconclusive with respect to this question in that both mechanisms would be expected to produce similar effects under the given circumstances. However, when the influence of the age of the discharge structure on the rate of optical degradation was noted it was realized that ultraviolet could also be ruled out as the primary mechanism. The ultraviolet output from the laser depends upon the instantaneous current-pressure conditions and should be independent of the previous history of the structure. The observed history dependence thus points unambiguously toward film deposition.

Before the ultraviolet is thrust completely aside it should be realized that this is indeed a real potential source of trouble. The ionized laser discharges, by their very nature, emit large quantities of ultraviolet light. Much of this is resonantly reabsorbed by the gas while a good part of the rest is attenuated by photo-ionization processes. Some ultraviolet, however, particularly in the far wings of the resonant lines, does arrive eventually at the optics. It is well known that ultraviolet can produce defects and color centers in crystals which would ultimately lead to a degradation of the laser performance. In fact, long term ultraviolet-induced solarizations of natural quartz windows of low-power ion gas lasers has been observed.⁴ We ourselves noted obvious solarization of a salt (NaCl) window used in one of our experiments. NaCl is, of course, particularly susceptible to the generation of ultraviolet-induced color centers. However, the synthetic quartz (Suprasil) used in these experiments never showed any sign of solarization under any conditions. This may be due to the amorphous nature of the material itself or to the fact that our windows and optics were always placed on the end of long tubes at relatively large distances from the active discharge region. This maximizes the probability that the ultraviolet will be absorbed by the unexcited gas between the discharge and the window or mirror. Placing the optics immediately adjacent to the discharge, without the benefit of the buffering gas layer, may lead to serious ultraviolet degradation of the optical components, and should be avoided as much as possible.

It was clear from the start that we were dealing with a surface degradation on the inner side of the window; the interferometric observations showing that only the inner side deformed, the restoration of the flat by surface cleaning techniques - abrasive, chemical and electrical, and the additional aging process required when a flat degraded on one side is reversed, all unambiguously indicated the presence of a surface film of some sort. The overall "aging" process associated with the damage phenomenon is consistent with a gradual buildup of a contaminating film.

Having established that an optical radiation absorbing layer forms on surfaces exposed to the ion laser discharge, the consequences of such a growth are predictable. At a given current level the windows tend to absorb more and more energy from the laser beam and to become increasingly lenticular. The direct insertion loss due to this absorption, which is too small to be detected by straightforward techniques, no doubt has little effect on the performance of the laser. However, the lenticular distortions of the Brewster-angle windows can have severe effects. The introduction of a lens-like element into the optical cavity can produce significant changes in the optical configuration leading to drastic alterations of mode size, number, and stability. Because the temperature distribution will roughly follow the laser mode pattern (although smoothed out) we see that near the center of the mode the window deformation has little effect on the modes. However, as we move off the laser beam symmetry axis, the inevitable temperature gradient produces deformations. The modes passing through these deformations are defocused and eventually suppressed. Thus, as the film absorption becomes significant, the first effect is a suppression of the modes on the outer edge of the laser beam and the observed beam pattern shrinks.

Actually because the windows are placed at Brewster's angle in optical cavity, strong astigmatic effects are produced. If a lens of focal length f_o is placed at the Brewster's angle with respect to a beam of light the focal lengths in the plane perpendicular to the axis around which the lens has been rotated is reduced to:

$$f_{\perp} = \frac{1}{(n+1) \cdot \sqrt{n^2 + 1}} f_o ,$$

which, for fused silica ($n \approx 1.463$), reduces to

$$f_{\perp} \approx 0.23 f_o .$$

In the plane parallel to the rotation axis the focal length becomes

$$f_{\parallel} = \frac{\sqrt{n_2 + 1}}{n + 1} f_0$$

$$\approx 0.72 f_0$$

Thus, the effects of the distortions are greatly magnified by the angle of the window, and we expect to see strong astigmatic effects since $f_{\perp} \sim 1/3 f_{\parallel}$. The modes in the plane corresponding to f_{\perp} are most strongly suppressed. As the distortion effects become stronger, the laser beam cross section becomes elliptical, and the long axis parallels the axis of rotation with an axis ratio of about three to one. This corresponds roughly to what is observed at intermediate damage levels.

Eventually, as the distortion phenomenon becomes even more severe, strong self-limiting effects set in. A well-established mode will distort the window precisely where it is most intense, which leads to strong de-focusing and hence increased loss for that mode. This tends to reduce the mode power, which alleviates the distortion a bit and a balance is established. The damaged window begins to act as an effective power limiter. No amount of increased input power can push the output power above this self-limited condition.

Under some conditions this self-limited situation can be temporally stable; more commonly, however, a dynamic instability occurs in which the spatial mode pattern breaks up into some complicated combination of higher-order modes which fluctuate rapidly with time. The modes are evidently not only defocusing themselves but actually turning themselves off, leading to a dynamic interaction between the fluctuating thermal distortions and the cavity mode.

Direct detection of this annoying film proved to be difficult. Given the extreme sensitivity of a laser optical cavity (to misalignment, etc.) and the poor thermal cooling of the internal surface of the window, the absorption required to produce a significant change in the performance of the laser is small indeed. In fact, even the most badly damaged windows produced completely negative results with most of the standard tests for thin films. Evidently the films are extremely thin. Visual inspection via a microscopic examination showed nothing; there were no fringes or interference colors evident, no increase in single pass optical absorption could be measured, and X-ray microprobe examination of the surfaces also showed nothing. One approach which appeared promising at first was the spectroscopic analysis of minute bits of material vaporized from the surface by a carefully focused

laser beam. However, the results (commercially obtained), while suggestive, proved unreliable in that certain easily identified elements which were known to be present were frequently not reported, thereby casting severe doubt on the remaining analysis.

Gradually it was realized that there were two somewhat unusual tests available which could provide reasonably reliable criteria for the existence of a contaminating film on the Brewster window: 1) the fluorescence observed through yellow filters commonly used for protection against the argon radiation and 2) the patterns of condensed moisture evaporating from a breath-fogged surface (the breath test). New undamaged windows consistently produced negative results for both tests. Damaged windows always showed both fluorescence and breath test patterns. During the cleaning of damaged windows, when the breath test indicated that the film had or had not been successfully removed, observation of the laser performance using the windows in question always confirmed this diagnosis.

There are several aspects that suggest that the films detected by the above methods are tightly bonded to the surface, perhaps in a metallic form since oxidation appears to be necessary to remove the film. Freshly damaged windows or those baked out in a vacuum environment proved not to be susceptible to nonabrasive cleansing techniques. Simply leaving them exposed to the air for several days or baking them in air led to easy and total restoration by means of the same previously ineffective nonabrasive techniques. This suggests conversion of the contamination to a less tightly bonded oxide form. Some sort of reactive bonding to the surface is also indicated by the fact that heating the window either directly or via the laser beam while exposed to the discharge generally led to higher damage rates. Heating the windows could hardly increase the deposition rate but could significantly enhance adsorption processes or chemical bonding surface reactions which might be going on. This additional effect of the laser beam on the surface film deposition is perhaps best illustrated by the "breath test" results on the mirrors. There was a general (disc-shaped) film where the mirror had been directly exposed to the discharge, as well as a clearly distinguishable secondary spot where the laser beam had been. There was evidently a general deposition of film, but the laser beam influenced the local character of this film.

Having established that an optically absorbing surface layer was being formed on the window surface exposed to the discharge, the next step was to determine how this layer developed and what was acting as the source or sources of the contamination. It is rather obvious that every component of the ion laser discharge structure must be considered a possible source of contamination. The well-known sputtering ability of the argon discharge and the inevitably high thermal loading of the structure can readily liberate particles and gases from the cathode, anode and bore. This has been abundantly confirmed by the X-ray microprobe analysis of the deposits which

had accumulated on the envelope walls of the several lasers used during the course of this contract. Such analysis yielded traces of no less than six elements from the cathode structure. It is clear that all nonessential materials and contaminants must be eliminated from the vacuum envelope. This is further emphasized by the observation that the presence of Apiezon H, low vapor pressure vacuum grease, near the window but not exposed to the beam, resulted in rapid film formation. This train of thought suggests that for the successful generation of very long life, high-power argon lasers the use of oil or mercury diffusion pumps during the processing should probably be avoided. We strongly recommend the use of vac-ion and/or cryo-vac systems exclusively.

The importance of good design and materials choice is equally obvious. Temperatures should be kept as low as possible, consistent with the over-all approach being employed. In the long run, the cathodes could prove to be quite troublesome for, in a gaseous atmosphere, ion bombardment of the cathode is inevitable. Some cathode heating and sputtering must always be present. The design of the cathode is therefore critical and should be carefully considered with respect to type, size, baffling, position, etc. As we will see later, the design of the anode is also important with respect to its influence on the transport of contaminants from place to place via plasma jet phenomena. Both electrodes are factors in the quest for long life and must be carefully designed.

In the particular case of the principal laser used in this contract study, the prime source of contamination proved to be the low vapor pressure vacuum grease used to mount the windows. The sudden improvement in performance when fused-on windows were used and the subsequent experiments with the deliberate introduction of Apiezon H grease inside the vacuum envelope, near the window, made this painfully obvious. The transport studies pointed out that the stopcocks were also probably contributing large amounts of grease. No doubt the cathode and bore erosion processes were adding further contaminants but these effects were thoroughly masked. This was, to say the least, disappointing but not without some consolation. Because of the greatly accelerated degradation rate, we were able to notice the phenomenon quite early and to conveniently study its properties.

To complete our grasp of the optical degradation problem it is important to understand the mechanisms by which the contaminants are transported from their point of generation, be it the cathode or bore or elsewhere, to the terminal optics. Much of the experimentation during the final quarter was designed to clarify these processes. At least three different effects must be considered: 1) ordinary diffusion of neutrals via thermal or concentration gradients, 2) gross mass transfer associated with the familiar gas-pumping phenomenon of ion lasers, and 3) the motion of charged species (particles or ions) under the influence of the plasma electric and magnetic fields (i. e., plasma jets, catephoresis, etc.)

Since our windows were mounted relatively far from the discharge region on the ends of cool tubes, it was difficult to understand how ordinary diffusion could be effective in transporting contaminants as far as the windows. There was too much cooled surface available for condensation; very little contaminant should reach the windows. An unsuccessful attempt to introduce a nitrogen cold trap between the discharge and the window confirmed the suspicion that diffusion was not a prime transport mechanism. In fact, the original interpretation given to this result was that it supported the ultraviolet hypothesis. There is, however, another possibility as we shall see.

There is a little question that the gas pumping effect can distribute contaminants throughout the system. The observed transport of sodium from the cathode of the principal laser through 2.5 meters of discharge bore to the anode bulb was probably due to this phenomenon. As is well known⁵ the gas is typically pumped toward the anode at low currents by the electron pressure but tends to reverse direction when the cathodic transport of ions toward the cathode begins to dominate at higher currents. This is therefore an efficient means of distributing "junk" throughout the system. However, because the gas flow doesn't penetrate far into the stagnant gas trapped in the tubes in front of the windows, gas pumping does not really explain how the film materials actually get all the way to the optics.

Suspecting some sort of charged particle transport, we began the series of experiments, described above, on the plasma found in the neighborhood of the optics. This led to the realization that there was a cold plasma and associated electric fields extending right up to the windows. At the anode end, in particular, negative particles are shot through the anode toward the window. A bright plume extending through the anode is a common observation in ion lasers. This is the same plasma jet phenomenon used in plasma torches. The clearly defined, cusp-like collection point of the artificially introduced contaminants reported above in the principal laser, as well as the violent ejection of carbon particles toward the anode window in the graphite laser, provided dramatic evidence of this jet-like behavior at the anode end.

The cathode end of the discharge typically lacks the bright plume and is much more subdued. The observed preferential degradation of the anode window over the cathode window is, no doubt, associated with this anode-cathode difference. That this should be so becomes clearer when it is realized that foreign particles injected into a plasma, particularly if they are of a macroscopic size, tend to become negatively charged and are thus pushed toward the anode end of the structure.

This happens for the same reason that the insulating walls always take on a negative charge. The condition that an insulating surface or any isolated object exposed to the plasma must satisfy is that no total current

be drawn to it. The electrons, with their higher mobility, reach the surface first, charging it negative until the rest of the electrons are sufficiently retarded and the ions accelerated that the equal current condition is achieved.

Macroscopic particles (e.g., vaporized carbon or grease) would therefore be negatively charged, swept down the bore, projected through the anode and kept centered in the tube by the negative walls. In this way they can bypass any cold trapping naturally present or deliberately introduced and drift down line of sight paths until they strike the terminal optics. This appears to be the dominant mechanism active in our lasers and can reasonably well explain all our observations at the anode end. The cathode end is more difficult to explain since the negative particles are accelerated away from the cathode. The positive ions which provide the laser action will be projected toward the cathode window, although the negative walls should be quite effective in trapping them. In our observations of the grease particle swarms, it was noted that occasionally a small fraction of the particles were observed to move in the opposite direction as if they were positively charged. This is not really understood at present but may be related to the propulsion effect of vaporized material being ejected from the particle under the action of the laser beam. More work on the details of contamination transport must be done. In any case, the degradation of the cathode window is always much slower than that of the anode window.

The identification of charged particle transport as the apparently dominant mechanism suggested that electric and/or magnetic counter measures might be extremely effective in controlling the optical degradation. In particular, the introduction of an independent rf discharge between the main discharge region and the window was found to be effective in restoring the damaged window and in inhibiting further degradation. The restoration effects are no doubt associated with mild rf sputter cleaning of the surface. The action of the rf in reducing the degradation rate is perhaps due to the fact that the continuous reversal of direction of the electric field in the rf discharge precludes the formation of any coherent, well formed plasma jet toward the window. Particles injected to the rf region from the anode of the main discharge will be trapped if the region is long enough that the transit time for injected charged particles is longer than the period of the rf. The anode end thus becomes much like the cathode and the anode window deposition rate should be reduced. By properly adjusting the rf configuration the deposition and sputter cleaning rates can be made to balance, potentially eliminating the lifetime limitations of contamination film degradation of the optics independent of the number or types of contamination sources which may remain within the discharge structure (for example, the cathode).

In summary, the results of this study clearly indicate the role of cleanliness in producing long-life, high power ion lasers. For very long-life performance the tube must be kept clean by careful design, choice of

materials and processing. The optics should never be mounted directly adjacent to the main discharge region as this greatly increases the possibility of ultraviolet damage and permits direct diffusion deposition of contaminants. The mirrors should be at the ends of reasonably long, cooled or adequately baffled tube to eliminate direct diffusion and to provide an ultraviolet attenuating layer of cooled gas between the window and the discharge. The cathodes which will inevitably suffer from ion bombardment, must be designed to reduce the surface loading as much as possible and to prevent the contaminants they release from finding their way into the main discharge region. This suggests that side-arm cathodes may be more effective in reducing optical degradation effects than in-line configurations. The anode should be designed to minimize the plasma jet phenomena. Processing of the system should probably involve the exclusive use of vac-ion and/or cryo-vac systems rather than oil or mercury diffusion pumps. And finally, remedial and preventative measures in the form of appropriate electric and/or magnetic fields can be applied in the region between the main discharge and the terminal optics; in particular, the rf discharge configuration described previously seems promising.

REFERENCES

1. Paananen, R. A.: Progress in Ionized Argon Lasers, IEEE Spectrum, Vol. 3, No. 6, June 1966, p. 97.
2. Bridges, W. B.; and Halsted, A. S.: Gaseous Ion Laser Research, AFAL-TR-67-89, Hughes Research Laboratory, Malibu, California, May 1967, Section VII, pp. 211-277.
3. Bridges, W. B.: Personal Communication.
4. Parker, J. V.: Metal Aperture Ion Lasers, Paper presented at the International Electron Devices Meeting, Washington, D. C., October 19, 1967.
5. Bridges, W. B. and Halsted, A. S.: Op. cit.

NEW TECHNOLOGY APPENDIX

A Method of Restoring Optically Degraded Laser Optics

A description of this innovation is presented on page 34 of this report.

A more detailed description will be forwarded with the Invention report at a later date, in accordance with the New Technology Clause of the contract.